LOW RADIOACTIVITY TECHNIQUES 2026 • YORK, UK

Backgrounds in the PICO Bubble Chambers

Mayank Tripathi

University of Chicago, for the PICO Collaboration

mtripathi@uchicago.edu

Dark Matter

- Galaxy rotation curves, gravitational lensing, and the CMB power spectrum independently point to a non-baryonic, weakly-interacting dark matter.
- Many candidates: WIMPs, Axions, Sterile Neutrinos, Sub-Gev Dark Sector ….
- Alternate Theories: SIDM, MOND….

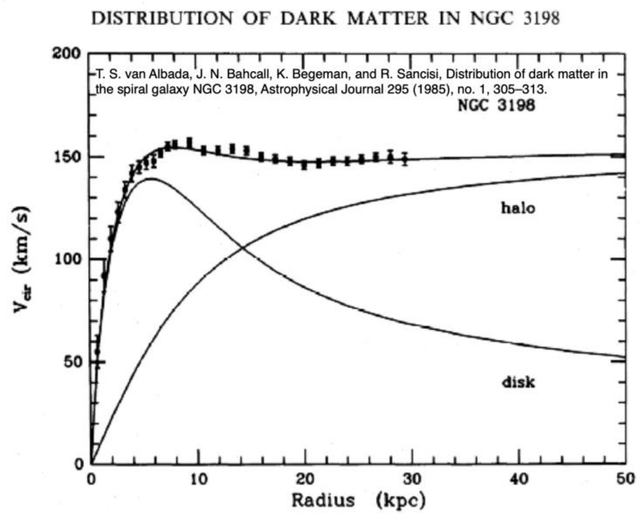

Credit: ESA/Hubble & NASA, S. Jha.

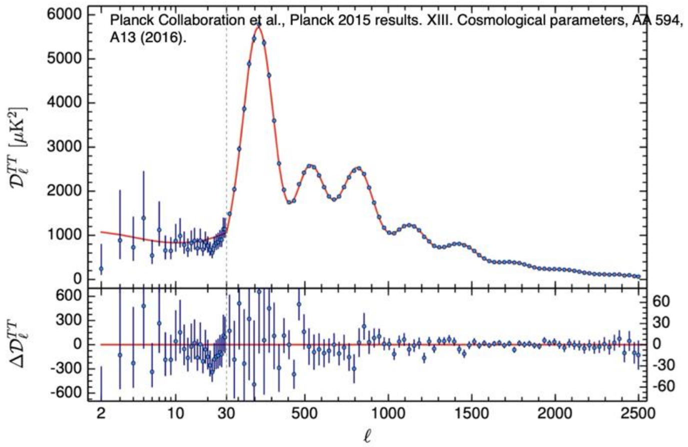

WIMPs & the Direct Detection Strategy

- A WIMP is expected to scatter elastically off a nucleus, depositing a tiny keV-scale recoil. Direct detection experiments are built to catch this signal.
- Expected rates are vanishingly small for weak-scale cross sections, so **experiments run deep underground - in ultra-radiopure materials**; to suppress cosmic rays and radioactive backgrounds.
- No single technology covers the whole parameter space: crystals, liquid-noble TPCs, and bubble chambers each bring different targets and different background-rejection strengths.

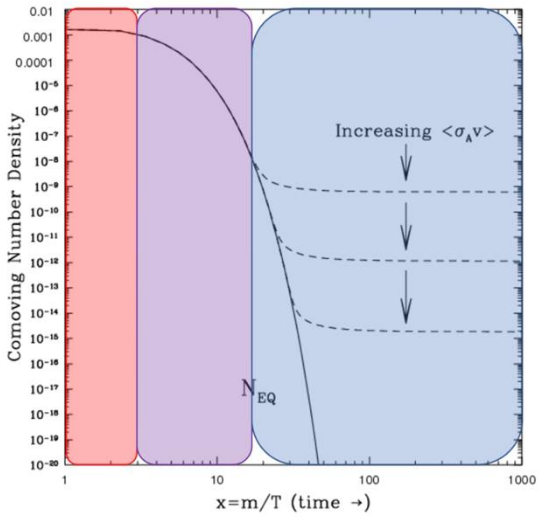

Thermal freeze-out sets the WIMP relic abundance for a given ⟨σv⟩.

~26%

of the universe's energy budget is dark matter (Planck 2015)

PICO's approach:

Superheated bubble chambers using fluorine-loaded target fluids, sensitive to spin-dependent WIMP-proton scattering, intrinsically insensitive to the dominant electron-recoil backgrounds.

PICO: A Bubble Chamber Dark Matter Search

- Located at SNOLAB: 6800 ft depth (6010 m.w.e.), one of the deepest labs in the world - **10^8 reduction in cosmic-ray flux.**
- Class-2000 clean room environment for radon and dust control.
- Superheated C_3F_8 target: sensitive to **spin-dependent WIMP-proton** coupling.
- Fluid can be swapped to probe different physics: C_3F_8 (SD), CF_3I (SI) and $C_2H_2F_4$ (low mass WIMPs) all offer different operating conditions and target nuclei.
- Every event is reconstructed in triple coincidence - acoustic, pressure, and optical channels.

$$\frac{d\sigma(E_R, v)}{dE_R} = \frac{m_T}{2\mu^2 v^2}\left(\sigma_0^{SI} F_{SI}^2(E_R) + \sigma_0^{SD} F_{SD}^2(E_R)\right)$$

$$\sigma_0^{SI} = \frac{4\mu^2}{\pi}\left[Z f_p + (A - Z) f_n\right]^2 \qquad \sigma_0^{SD} = \frac{32 G_F^2 \mu^2}{\pi}\frac{J+1}{J}\left[a_p\langle S_p\rangle + a_n\langle S_n\rangle\right]^2$$

SNOLAB, Sudbury, Canada – underground campus

What Is a Bubble Chamber and How Does It Work?

- Target fluid is held under pressure, just below its boiling point in a liquid state.
- Lowering the pressure creates a metastable superheated state.
- The detector stays in the superheated state until an energy deposition above the Seitz threshold (3.29 keV) in a critical radius nucleates a bubble, governed by Seitz's "Hot Spike" model.
  - Threshold can be tuned by P, T.
- **Electron recoils deposit energy too diffusely to concentrate enough within the critical radius - they simply can't nucleate. No analysis cut required.**
- Cameras catch the bubble and data is recorded, then fast pistons recompress the chamber to start the next cycle.

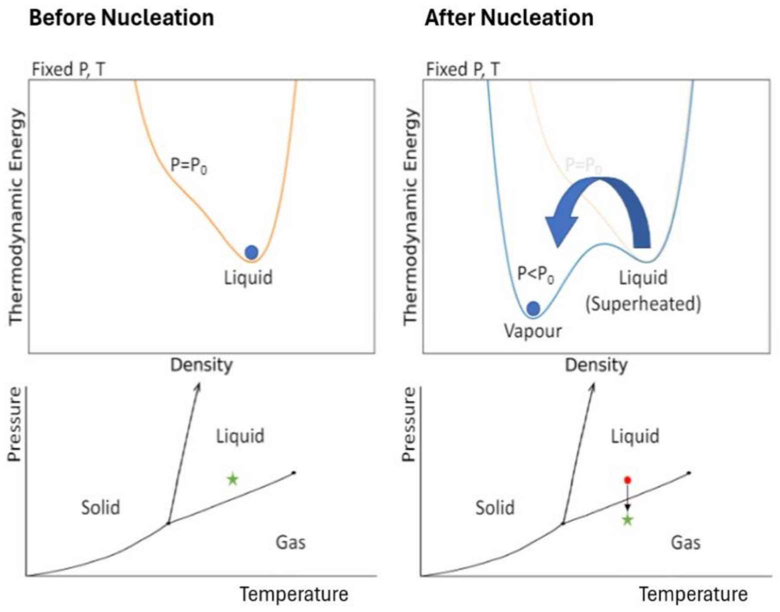

$$r_c = \frac{2\sigma}{P_b - P_l}\,.$$

Form the surface of a sphere | Convert liquid to sphere of vapour | Work done by expanding gas

$$Q_{\mathrm{Seitz}} = 4\pi r_c^2\left(\sigma - T\frac{\partial\sigma}{\partial T}\right) + \frac{4\pi r_c^3}{3}\rho_b(h_b - h_l) - \frac{4\pi r_c^3}{3}(P_b - P_l)$$

A nucleated bubble, imaged by the camera system.

Why Bubble Chambers?

1 **Fluorine = SD sensitivity**

Freon-based fluids (C_3F_8) give outstanding spin-dependent WIMP-proton sensitivity in the relevant mass range.

2 **Swappable targets**

C_3F_8 (SD), CF_3I (SI), and $C_2H_2F_4$ (low-mass WIMPs) probe different parameter space with different operating conditions.

3 **Blind to electron recoils**

The dominant background at most underground labs is suppressed by physics, not an analysis cut.

4 **Stable at scale**

Demonstrated background-free operation with excellent nuclear-recoil response across four hardware generations.

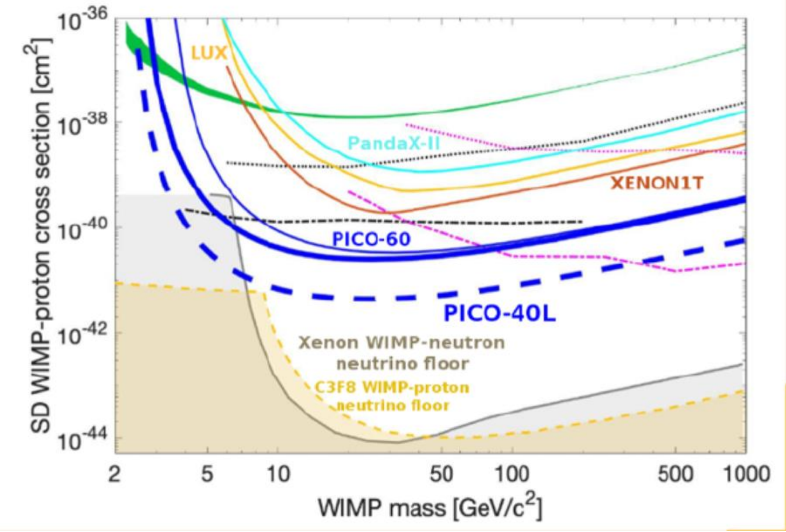

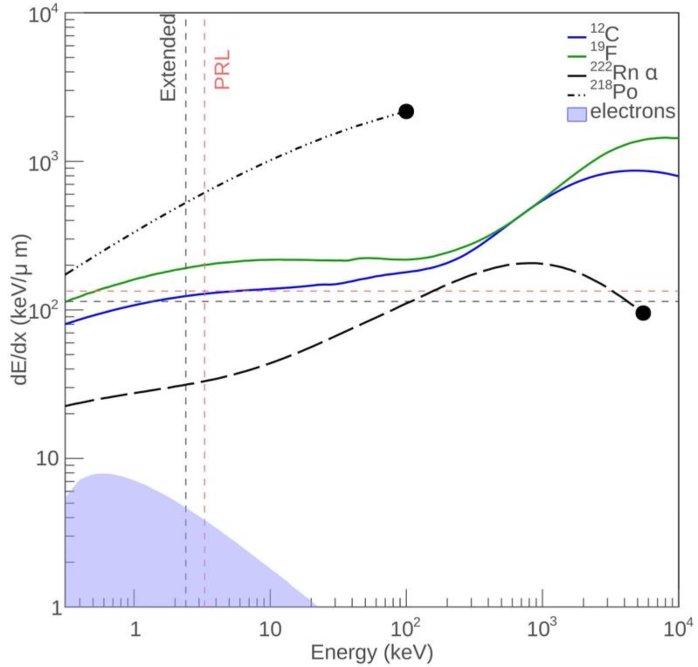

Four Generations of PICO Bubble Chambers

Same core physics - superheated C_3F_8 - carried across four hardware generations, each re-engineered to cut backgrounds and scale fiducial mass: 2 L → 35 L → 35 L (RSU) → a projected 260 L.

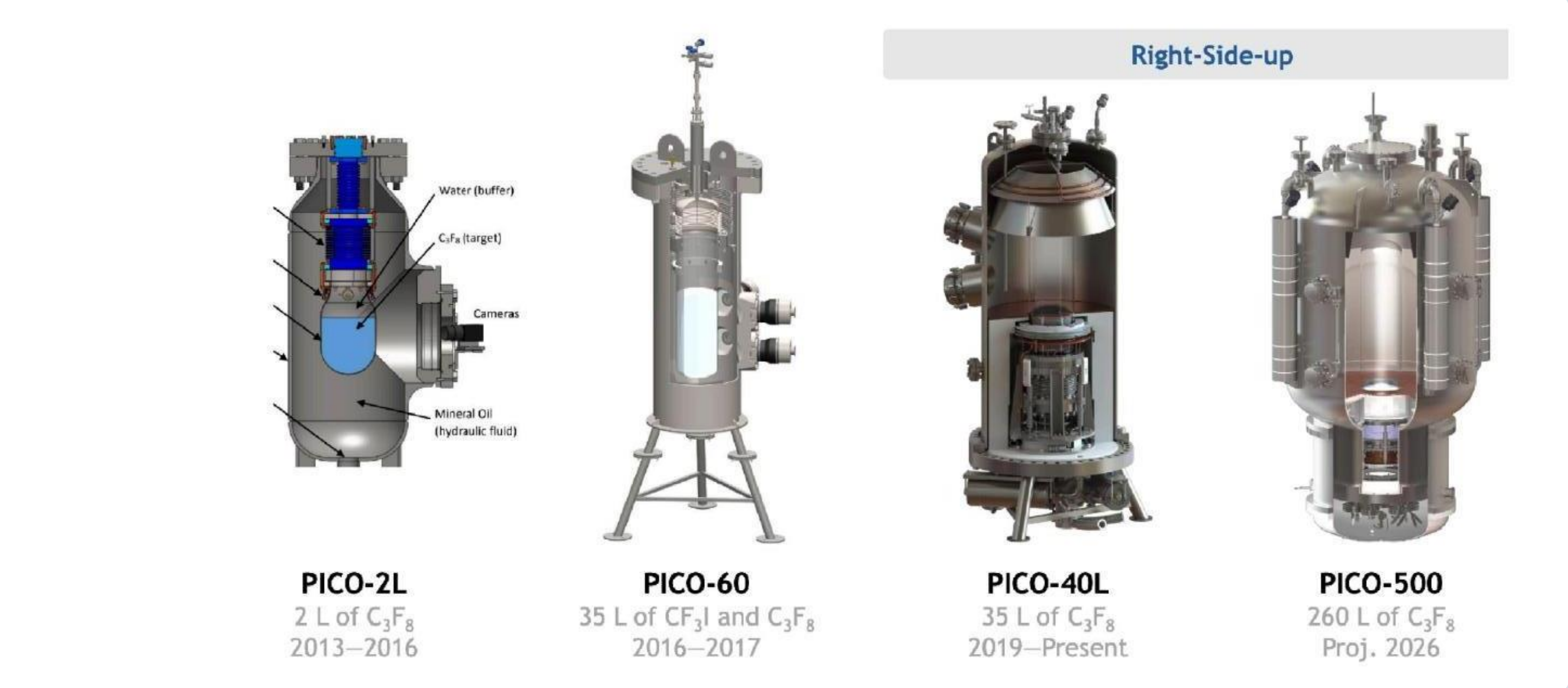

The Problem With the Upside-Down Design

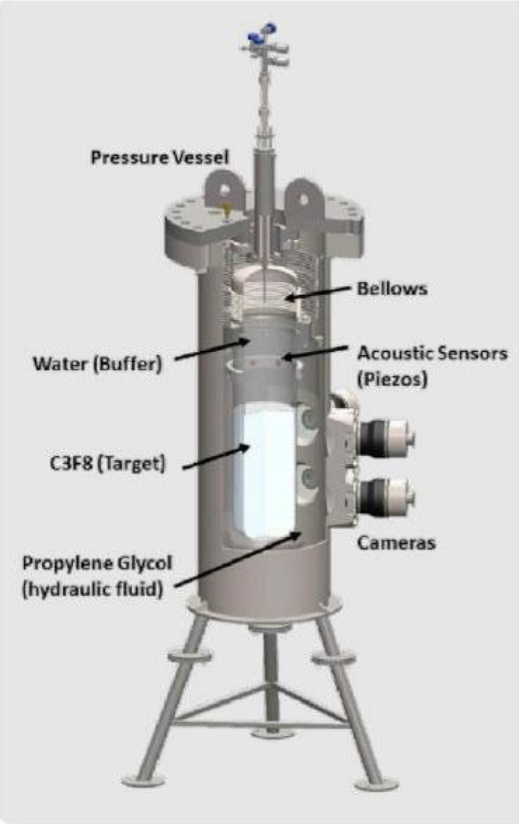

Original geometry: bellows above the C_3F_8 target.

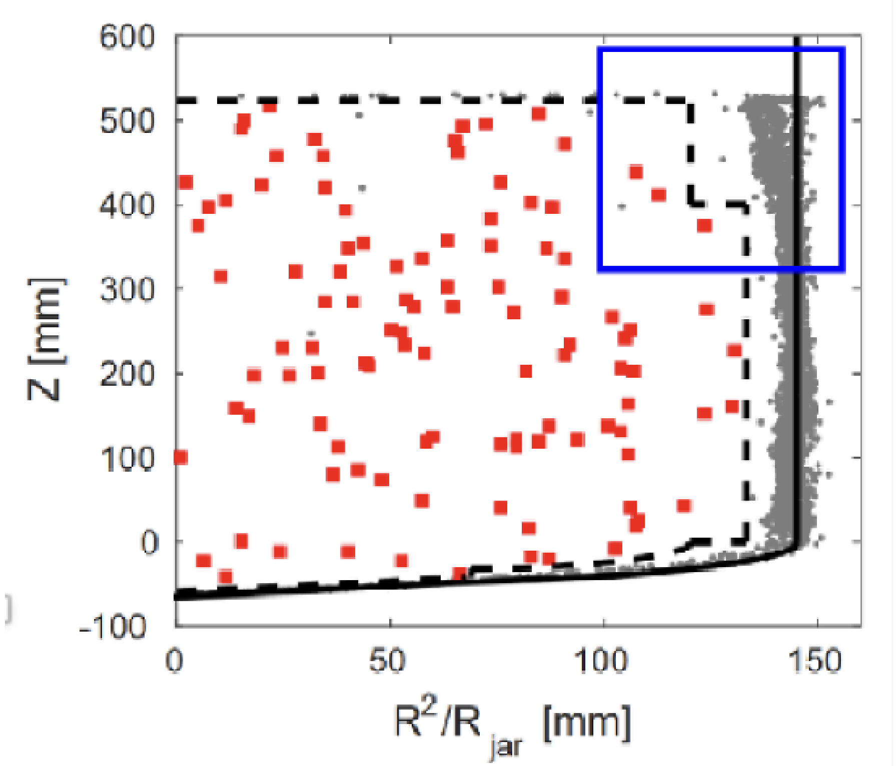

- Bellows sat above the water buffer, in direct line with the target.
- Particulates shed from the buffer water drove up wall-nucleation rates.
- Particulates could also settle at the bottom of the jar in fiducial volume - a background source that grows over time.

The Fix: Right-Side-Up (RSU)

PICO-40L in the right-side-up (RSU) configuration.

- **Inverted geometry:**
  - bellows moved to the bottom, buffer liquid eliminated.
- **Quartz inner jar:**
  - introduced to compress the C_3F_8 target liquid.
- **Hot region:**
  - establishes superheat in the C_3F_8.
- **Cold region:**
  - keeps C_3F_8 in contact with the bellows cold , preventing boiling there.
- **PICO-40L is the first large-scale implementation of RSU design - a proof-of-concept for PICO-500.**

PICO-40L: The Right-Side-Up Design

Located at SNOLAB, running since 2023: two quartz jars connected by bellows compress the C_3F_8 target in a right-side-up (RSU) configuration, with a temperature gradient across the bellows to avoid unwanted nucleation there.

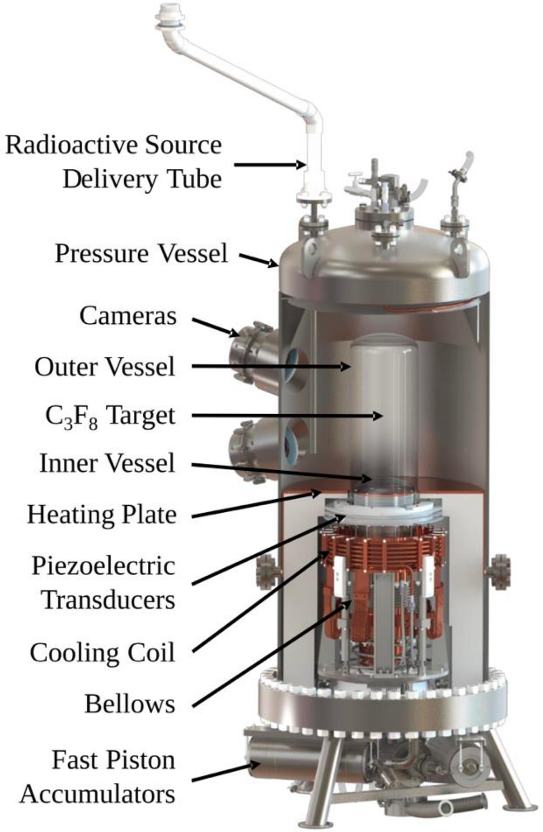

The assembled inner detector as installed underground at SNOLAB.

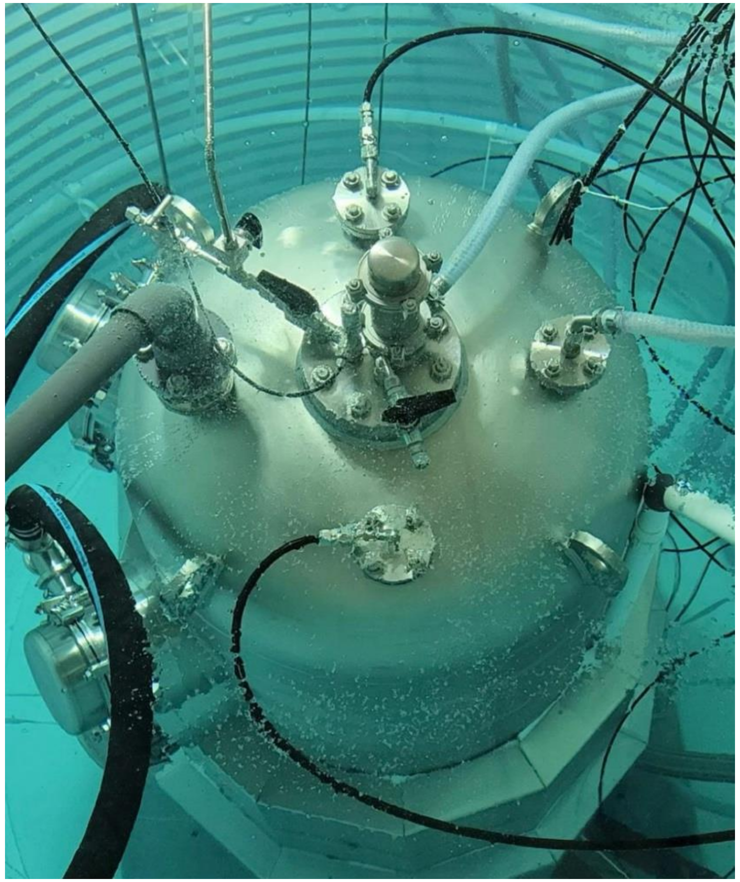

The PICO-40L pressure vessel submerged in UPW.

1 Backgrounds in PICO

Material screening → underground handling → detector-level rejection → the total budget

Screening the Fused-Silica Jars

- The C_3F_8 target sits in a fused-silica jar - among the largest ever made for a bubble chamber - so its intrinsic U/Th content sets a direct background floor.
- Crushed sample assay: representative jar material is crushed and screened to bound bulk U/Th/K contamination.
- Results feed directly into the material background budget shown later in this talk.

PICO-40 Measurement

Sample Description	Manufacturer	Mass (g)	Live Time (days)	Counting Dates (if applicable)		238U from 226Ra	238U from 234Th	235U	232Th	40K	137Cs	60Co	Comments
PICO 97	Heraeus PN 93800 SUP 300 Order # 1701566 Charge # 17045510	56.8 g	9.673	May 17, 2019	(mBq/kg)	<9.39	77.30 +- 172.90	9.36 +- 9.80	<10.15	<72.41	8.88 +- 6.87	<3.98	
Fused Silica Synthetic Quartz	Made on 12/11/17			May 27, 2019	(ppb or ppm)	<0.59 ppb	6.26 ppb +- 14 ppb	16.47 ppb +- 17.25 ppb	<2.5 ppb	<2.34 ppm			

PICO-500 Measurement

PICO CW53	LTD Materials LLC	4.994 g	40.055	251202	Dec 2, 2025	Results:	238U from 226Ra	238U from 234Th	235U	232Th	40K	137Cs	60Co	Comments
HSQ-900 Synthetic Quartz (Polished)	Polished HSQ 900 Sample disks				Jan 9, 2025	(mBq/kg)	<5.06	<32.70	1.34 +- 1.12	<12.77	395.98 +- 264.70	<83.66	<9.03	
	One disk crushed into a powder and placed into the standard Fisher Vial					(ppb or ppm)	<0.41 ppb	<2.65 ppb	2.36 ppb +- 1.97 ppb	<3.14 ppb	12.79 ppm +- 8.55 ppm			
						Results:	210Pb:	7Be:	54Mn:	228Ac:				
						(mBq/kg)	<360.60	<88.92	<13.12	17.20 +- 11.19				
						(ppb or ppm)	<29.21 ppb			4.23 ppb +- 2.75 ppb				

Component-by-Component Screening

Component	Events per Live-Year	90% CL UL
Nuclear Recoils		
Radiogenic neutrons		
Mineral Oil	—	0.697
Pressure Vessel	$0.145^{+0.080}_{-0.074}$	0.249
Inner Cu Disk	$0.100^{+0.110}_{-0.099}$	0.242
Outer Cu Plate	$0.086^{+0.096}_{-0.085}$	0.211
Lower Retroreflector	$\left(9.7^{+1.2}_{-1.1}\right) \times 10^{-3}$	1.13×10^{-2}
Thermal Insulation	—	9.87×10^{-3}
Cameras	$\left(3.88^{+0.47}_{-0.45}\right) \times 10^{-3}$	4.50×10^{-3}
Piezoelectric PCB	$\left(7.6^{+10.0}_{-2.5}\right) \times 10^{-4}$	2.11×10^{-3}
Upper Retroreflector	$\left(1.81^{+0.22}_{-0.20}\right) \times 10^{-3}$	2.09×10^{-3}
Outer RTDs	$\left(2.91^{+0.83}_{-0.78}\right) \times 10^{-4}$	3.99×10^{-4}
LED	$\left(5.39^{+0.71}_{-0.67}\right) \times 10^{-5}$	6.33×10^{-5}
Inner Quartz Jar	$\left(3.5^{+1.7}_{-1.6}\right) \times 10^{-5}$	5.70×10^{-5}
Camera PCB	$\left(9.3^{+18.0}_{-3.7}\right) \times 10^{-6}$	3.37×10^{-5}
Quartz Lens	$\left(1.40^{+0.64}_{-0.61}\right) \times 10^{-8}$	2.21×10^{-8}
Radiogenic subtotal	$0.72^{+0.34}_{-0.32}$	1.14
Cosmogenic Neutrons	—	0.1
CEvNS	$1.38^{+0.37}_{-0.33}$	1.86
Total NR	$\mathbf{2.17^{+0.49}_{-0.47}}$	**2.80**
Electron Recoils		
Internal	$0.006^{+0.046}_{-0.006}$	0.097
External	$0.047^{+0.354}_{-0.043}$	0.738
Total ER	$\mathbf{0.054^{+0.400}_{-0.048}}$	**0.837**
Total singles	$\mathbf{2.35^{+0.69}_{-0.53}}$	**3.38**

PRELIMINARY

- Every material in the detector - mineral oil, copper hardware, retroreflectors, RTDs, camera parts, piezo components - is individually screened.
- Each measured activity converts into a predicted single-bubble background rate for that component.
- **Dominant terms: copper hardware (inner disk, outer plate).**
- Retroreflectors, RTDs, cameras, and piezo parts each contribute far less.
- **Combined material background: < 1.14 single-bubble events / live-year.**

Radon Mitigation: Continuous N_2 Purge, Assembly to Installation

All wetted surfaces are kept inside nitrogen-purged bags from the moment the jars are assembled until the vessel is closed underground - continuously flushing dust before it can plate out on critical surfaces.

- Outer & inner jar bagged in custom **aluminum bags**.
- Continuous N_2 flow through dedicated gas bulkheads.
- Radon concentration around the jar is reduced from 130 Bq/m^3 to ~2 Bq/m^3.

Daily monitoring, all stages: LN_2 dewar level & flow-rate logs • inter-jar vacuum checks • cleanroom particulate counts

Vessel Cleaning

- All wetted surfaces (pressure vessel, inner jar, plumbing) are cleaned before assembly to remove dust deposits that would otherwise drive wall-nucleation rates.
- Cleaning is performed in the Class-1000 cleanroom to avoid re-contamination between cleaning and assembly.
- Inner vessel (housing active fluid) cleaned with UPW underground.
- Outlet filter is photographed under microscope and run through an algorithm to get particulate count.
- Cleaning and Particulate background paper is being prepared for submission to JINST.

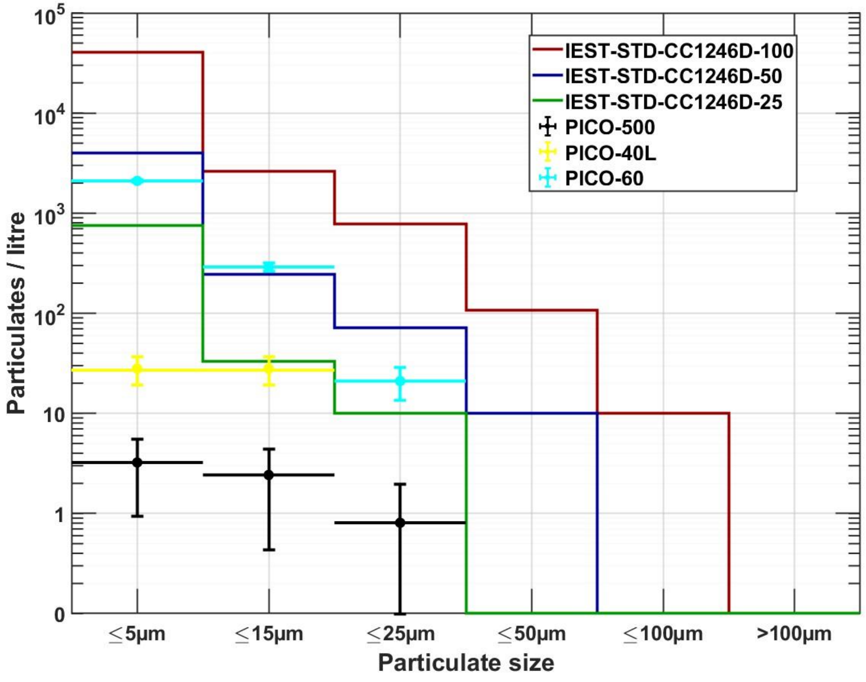

Radon Assay: Technique & Preliminary Result

- Rn-222 emanation from the PICO-500 fused-silica vessels is measured with a low-pressure gas emanation assay: samples emanate for 5–20 days, then are drawn through a hybrid pre-concentration trap and counted on a calibrated Lucas-cell alpha system.
- Flow rate and trap mass are tuned so the charcoal trap's breakthrough time comfortably exceeds the counting period - no radon escapes uncaptured during the assay.
- Preliminary measurement on the outer fused-silica vessel gives an emanation rate of order 0.1 Bq/m² - consistent with keeping the radon-chain contribution within the ≤0.1 events/year background budget target for PICO-500.
- Assay campaign is ongoing to build statistics on additional vessel surfaces and finalize systematics ahead of the PICO-500 background budget.
- PICO-500 Radon assay and hybrid trap paper in preparation.

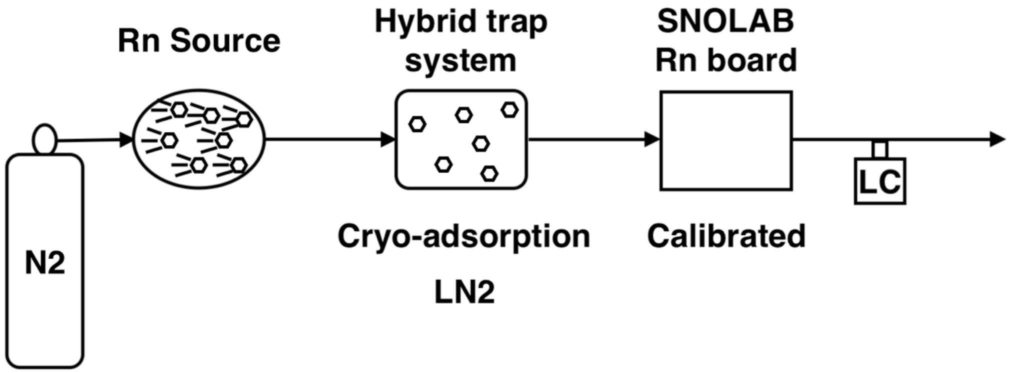

Assay chain: emanation → hybrid trap (cryo-adsorption) → calibrated counting.

Preliminary — PICO internal analysis, subject to collaboration review.

Rejecting Backgrounds I: The Optical Channel

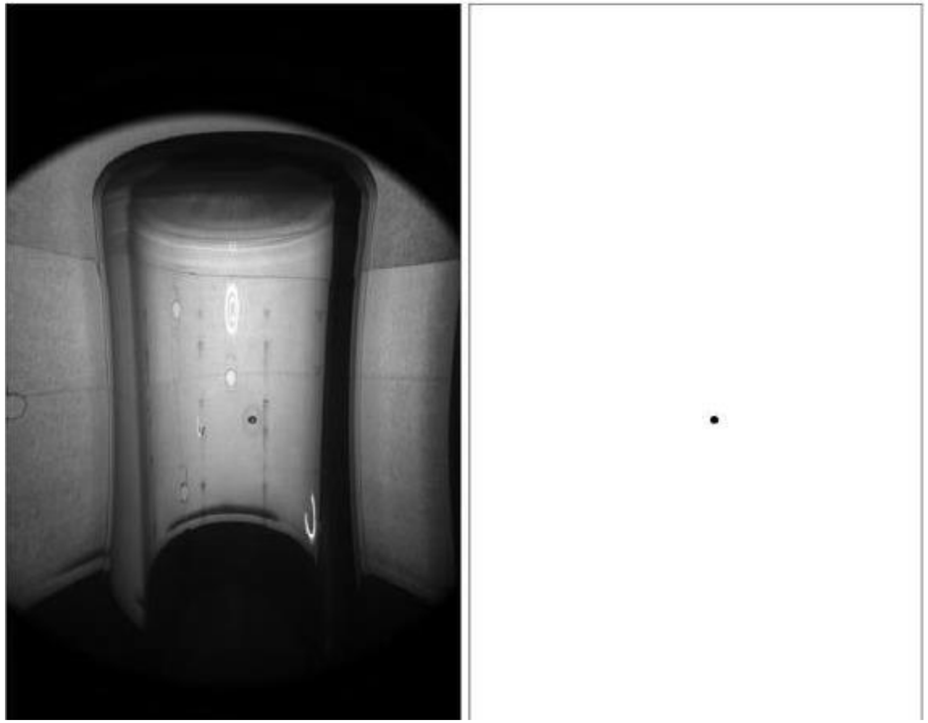

Raw fisheye frame: a bubble appears as a bright glint. After Processing, reduced to a single (x , y) position.

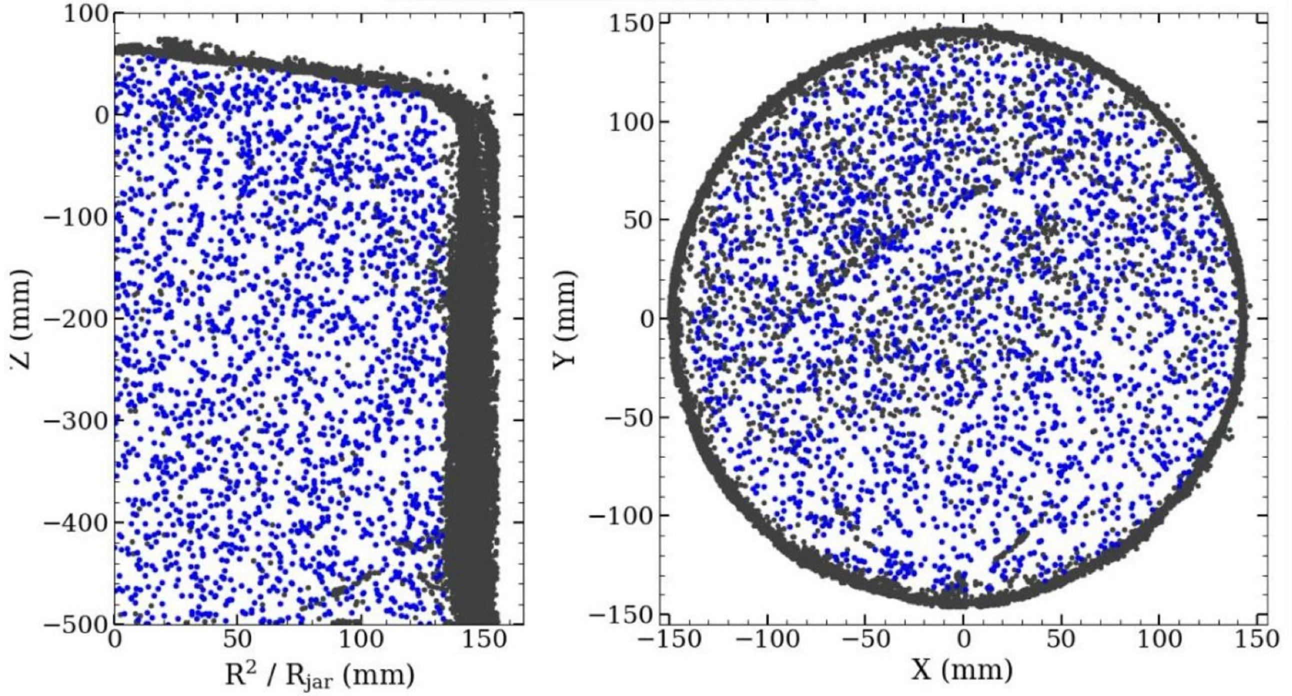

Z vs. R^2/R_{jar} and X vs. Y across many events: stereoscopic imaging gives ~1 mm resolution and defines the fiducial volume.

- Four cameras provide stereoscopic imaging, reconstructing the (x, y, z) vertex of every bubble to ~1 mm resolution.
- **Position reconstruction separates bulk (fiducial) events from wall-nucleated events, which cluster at high R^2/R_{jar}.**

Rejecting Backgrounds II: The Pressure Channel

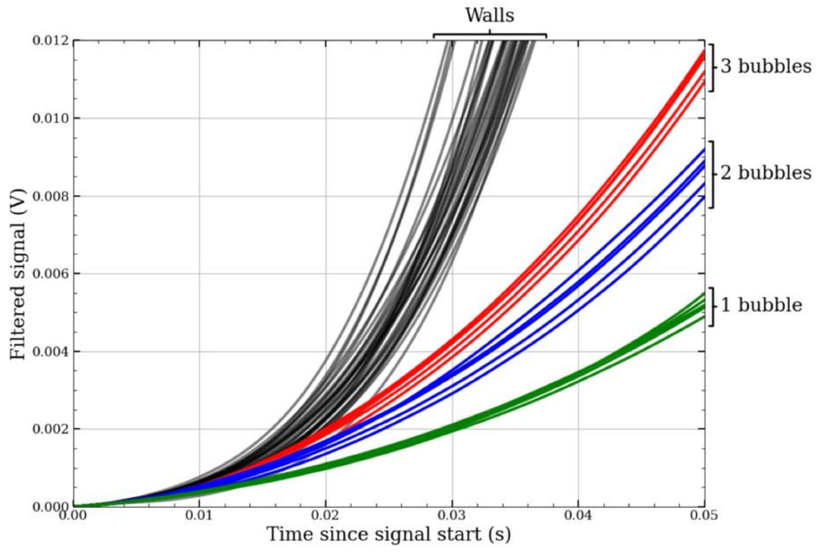

Filtered Dytran signal for 1, 2, and 3 bubbles — pressure rise scales with bubble multiplicity.

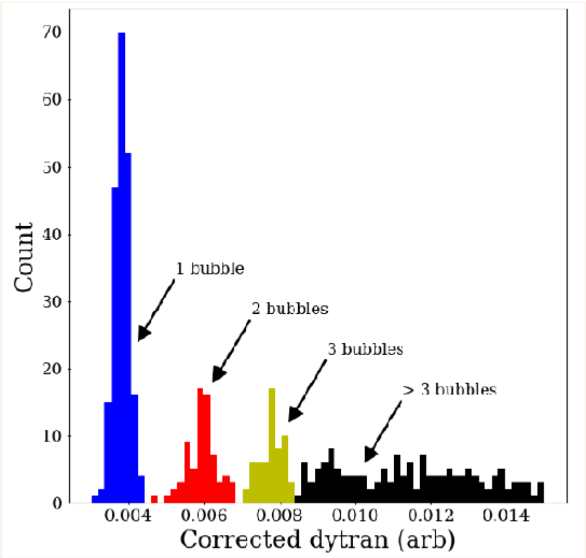

Corrected Dytran amplitude: single/double/triple(+) bubble populations resolve into distinct peaks.

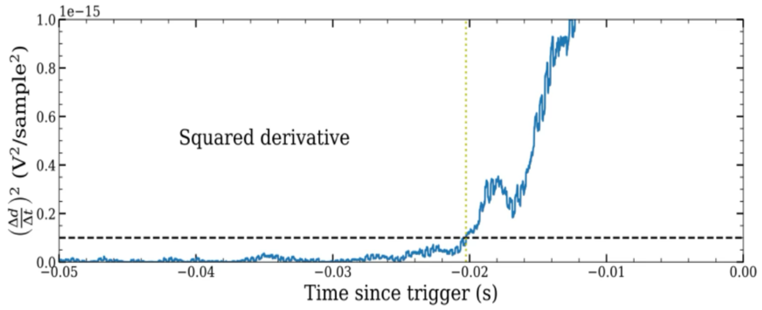

- A fast pressure transducer (Dytran) measures the transient pressure variations over time as each bubble forms (dP/dt).
- Pressure change over time is greater for events in which multiple bubbles nucleated.
- The corrected Dytran amplitude gives precise single bubble counting - **a WIMP candidate must be single-bubble**, since multi-bubble events are overwhelmingly neutron-induced.
- The rising edge of the pressure trace also fixes the event start time (T0).

Rejecting Backgrounds III: The Acoustic Channel

Piezoelectric transducers.

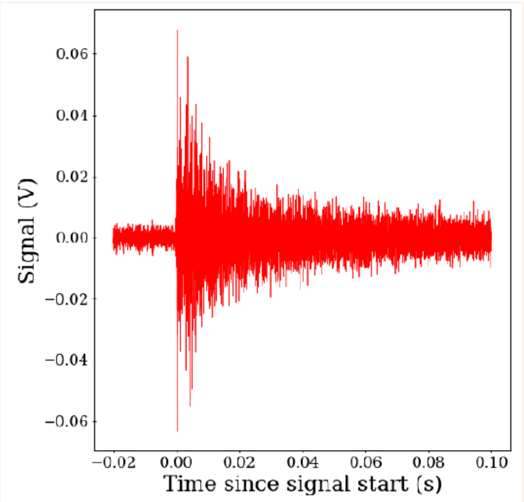

Raw piezo signal - 12 sensors record the acoustic wave from a forming bubble.

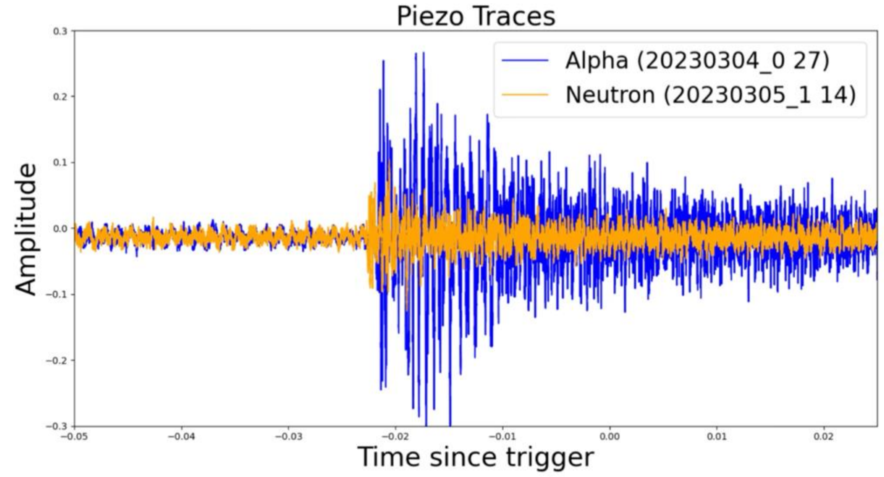

Raw piezo signal of an alpha induced single bubble event and neutron induced single bubble event

- 12 piezoelectric acoustic transducers at the bottom of the jar record the pressure wave radiating from a nucleating bubble.
- Alpha particle create many micro bubbles along a short train which merge to create one louder macroscopic bubble.
- In contrast, a neutron deposits heat locally to nucleate a bubble.
- **Alphas ring far louder (an audible “plink”) than neutron-induced nuclear recoils.**

Rejecting Backgrounds IV: The Acoustic Parameter

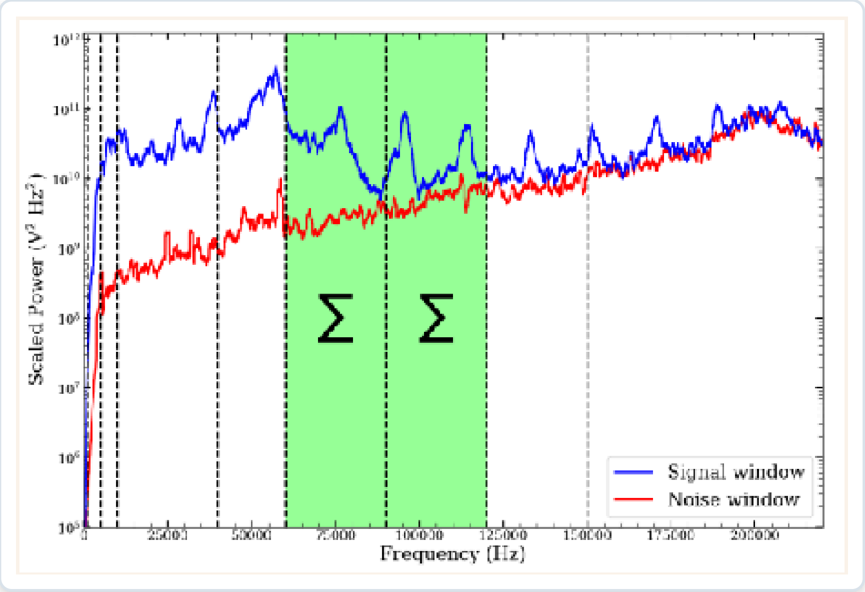

FFT power spectrum: signal (blue) vs. pre-trigger noise (red); green bands enter the AP sum.

$\mathcal{S}$, (Equation 4.2).

$$\mathcal{S}_{p,b} = \sum_{i=f_{b,1}}^{f_{b,2}} \mathrm{psd}_i f_i \qquad (4.$$

$$\mathcal{R}_{p,b} = \mathcal{S}_{p,b} - \mathcal{N}_{p,b} \qquad (4.$$

Where $f_{b,1}$ and $f_{b,2}$ are the edges of the frequency bands, psd_i is the PSD for ba i, p represents the piezo number, and b represents the band number.

$$AP = \frac{\sum_p \sum_{b=0}^{8} G(b) \mathcal{R}^*_{p,b}}{\sum_p \sum_{b=0}^{8} G(b)}$$

AP calculation

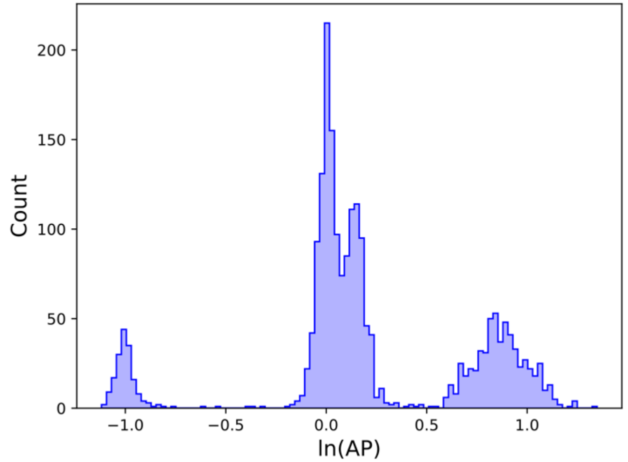

Resulting AP distribution: three well-separated populations by acoustic loudness.

- The raw signal is Fourier Transformed; per-piezo, per-frequency-band residual power (relative to pre-trigger noise window) is summed into a single Acoustic Parameter (AP) per event.
- AP tracks interaction energy – **alphas (high dE/dx) ring far louder than neutron-induced nuclear recoils**, giving powerful particle discrimination.

Alpha Spectroscopy: A New Bubble-Chamber Tool

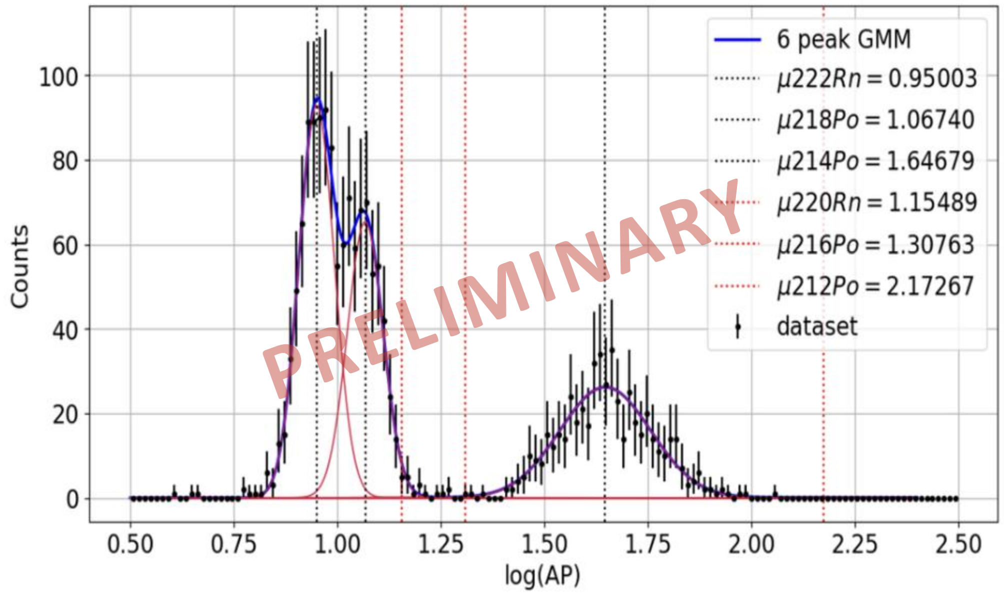

Figure 5.14: 6-peak Gaussian mixture model fitted to the log(AP) histogram alpha data using the Levenberg–Marquardt method. The complete fit is plotted in blue, with the individual Gaussian distributions shown in red. 95% Poisson confidence intervals were used as error bars.

Credit: E. Adams Thesis, Alpha Spectroscopy in a Superheater Bubble Chamber and the design of the PICO-500 Hydraulic Control Cart

- **First in-situ acoustic alpha spectroscopy performed in a bubble chamber — tuning AP on neutron calibration data, then focusing on alphas, resolves individual U/Th-chain decay lines directly from science data.**
- Beyond the physics result, it's a built-in radioassay tool: PICO can fingerprint its own U/Th contamination without a dedicated screening campaign. Paper in preparation.

Backgrounds: Alphas, Neutrons, Electron Recoils

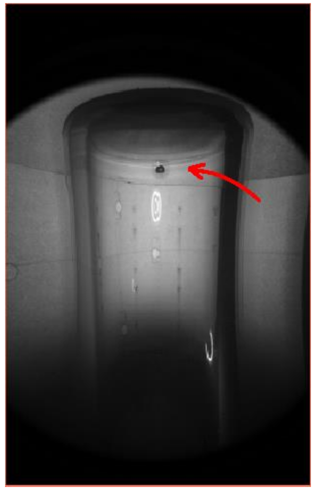

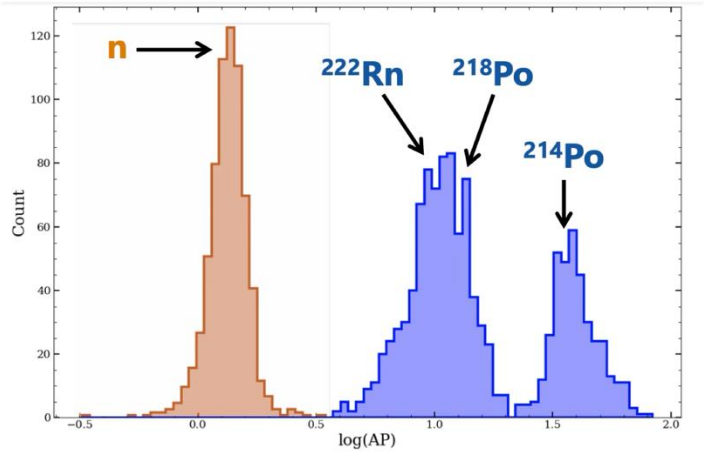

Alphas: single, unmistakably bright bubble.

Neutrons: nuclear recoils, frequently multi-bubble.

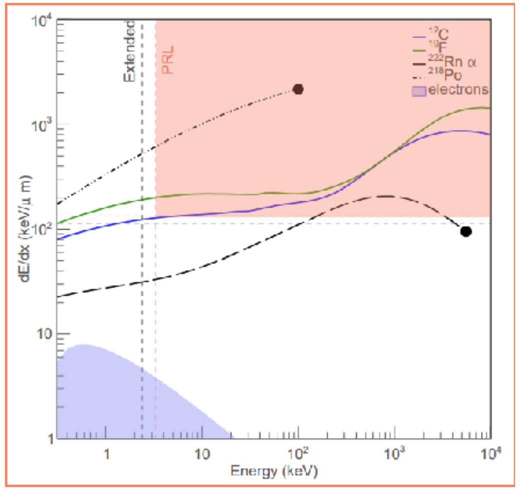

Electron recoils: dE/dx (shaded) sits far below the nuclear-recoil/Seitz curves — ERs essentially never nucleate.

- Acoustic loudness (AP) is used to discriminate alpha induced single bubble and neutron induced single bubble. Alpha particles deposit higher energy than neutron (audible plink)
- Neutrons undergo nuclear recoils and produce single and multiple bubble in ratio of 1 : 3.3.
  - 6010 m.w.e shielding, large water tank around around pressure vessel additional cosmogenic neutron shielding
  - Radiogenic neutrons reduced by careful selection of materials
- Electron recoils are suppressed by physics. They simply can't concentrate enough energy within the critical radius to nucleate at PICO's operating thresholds.
- **A WIMP candidate must be single bubble, neutron-like acoustically, inside the fiducial volume.**

PICO-500: Status & Timeline

PICO-500 must be assembled underground at SNOLAB.

The silica jar, wrapped for low-background installation.

- Lessons learned from PICO-40:
  - The RSU design works and can be used effectively to run a dark matter experiment at scale.
  - Temperature control across the bellows is tricky, but ultimately doable with careful engineering.
  - A dedicated PICO-40L detector paper is coming out soon.
- PICO-500 will use 250 L of C_3F_8 target fluid - largest silica jar ever made for a bubble chamber.
- Same right-side-up (RSU) mechanical design validated by PICO-40L, scaled up rather than re-engineered - de-risked by the 40L proof-of-concept run.
- Construction well underway; detector systems (instrumentation, electronics) to be installed later this year.
- Radon emanation assay analysis is underway to characterize backgrounds ahead of fill.
- **Timeline: fluid fill in early 2027, commissioning mid-to-late 2027.**

Conclusion

- **Bubble chambers can be made effectively insensitive to** electron recoils.
- Fluorine loaded target fluids give excellent spin-dependent WIMP-proton sensitivity; acoustic, pressure and optical channels together provide powerful, redundant background discrimination.
- **The right-side-up design works**: bellows below the target, buffer liquid gone.
- **Backgrounds are controlled in layers**: screening, N_2-purged handling, cleaning and radon assay hold the material term below 1.14 events/live-year.
- **Three channels must agree** on a WIMP candidate: bulk position, a single bubble, neutron-like acoustics.
- **Acoustics now measure, not just veto**: the first in-situ alpha spectroscopy in a bubble chamber resolves U/Th-chain lines from science data.
- **PICO-500 is next**: 250 L of C_3F_8 in the same validated geometry, fill in early 2027 and commissioning mid-to-late 2027.

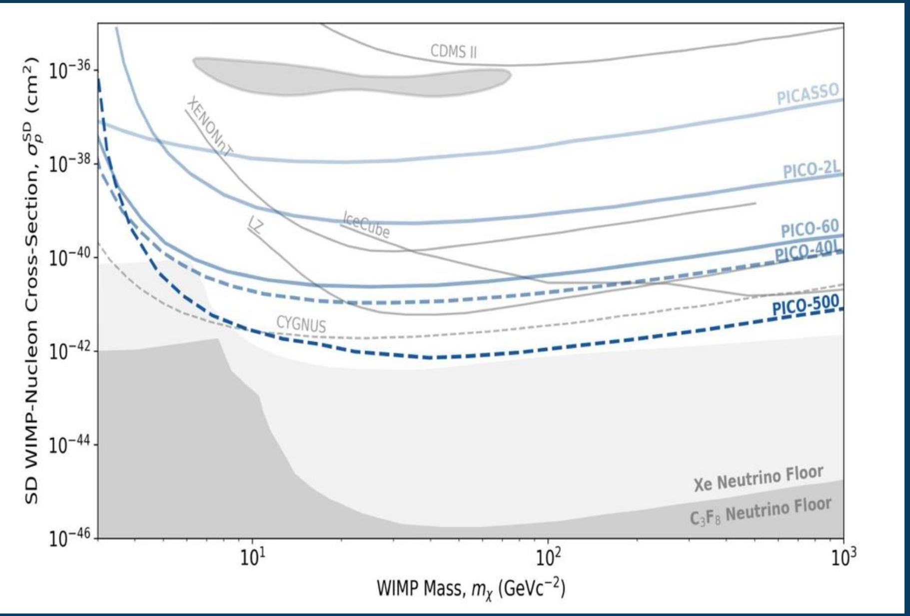

Spin-dependent WIMP-proton limits: PICO-60, PICO-40L, and the PICO-500 projection.

The PICO Collaboration

Thank you - and thanks to the many collaborators whose plots and figures appear throughout this talk.

PICO experiment

- PICO experiment is located at SNOLAB in Sudbury, Canada.
    - Located at a depth of 6800 ft (6010 m w.e), SNOLAB is one of the deepest labs in the world.
    - Class 2000 clean room environment.
    - 10^8 **reduction in μ flux.**
- PICO collaboration operates a bubble chamber filled with C_3F_8 target fluid and is sensitive to spin dependent WIMP-proton (neutron) cross section.
    - Spin independent cross section $\propto A^2$. Ar, Ge, Xe preferred.
    - **Good candidates for WIMP-proton spin dependent targets include H, Fl, Al, Nb.**
    - Good candidates for WIMP-neutron targets include Ge, Xe.

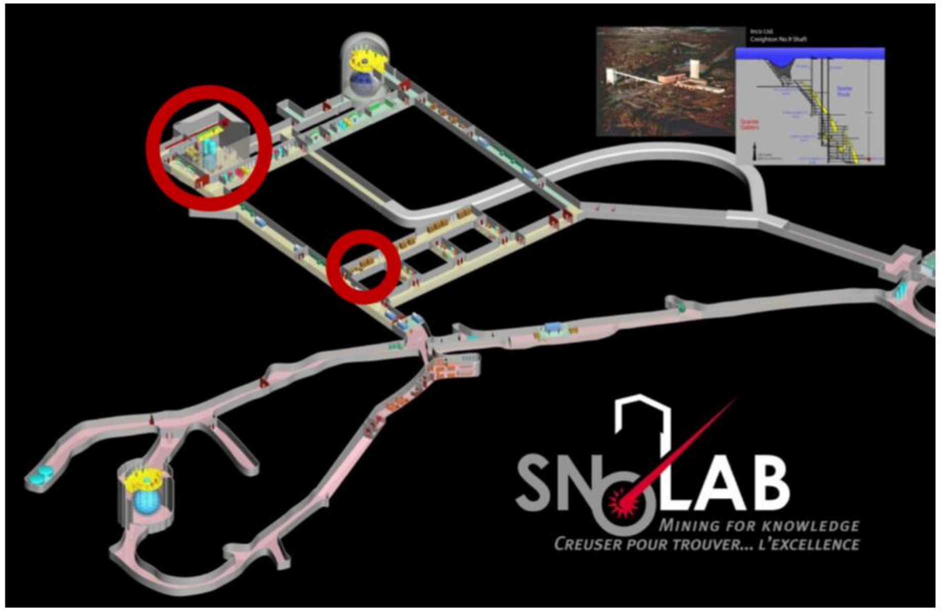

$$\frac{d\sigma(E_R, v)}{dE_R} = \frac{m_T}{2\mu^2 v^2}\left(\sigma_0^{SI} F_{SI}^2(E_R) + \sigma_0^{SD} F_{SD}^2(E_R)\right)$$

$$\sigma_0^{SI} = \frac{4\mu^2}{\pi}\left[Zf_p + (A-Z)f_n\right]^2 \qquad \sigma_0^{SD} = \frac{32 G_F^2 \mu^2}{\pi}\frac{J+1}{J}\left[a_p\langle S_p\rangle + a_n\langle S_n\rangle\right]^2$$

Detection Principle: Superheated Fluid

- Target fluid held just below its boiling point, in a metastable superheated state.
- A nuclear recoil deposits energy that seeds a vapor bubble (Seitz "Hot Spike" model).
- Bubble grows only if recoil energy exceeds the Seitz threshold Q_{seith} within the critical radius rc — a tunable knob via chamber pressure and temperature.
- Electron recoils deposit energy too diffusely to nucleate at these operating conditions — PICO is intrinsically blind to the dominant ER backgrounds, no analysis cut required.

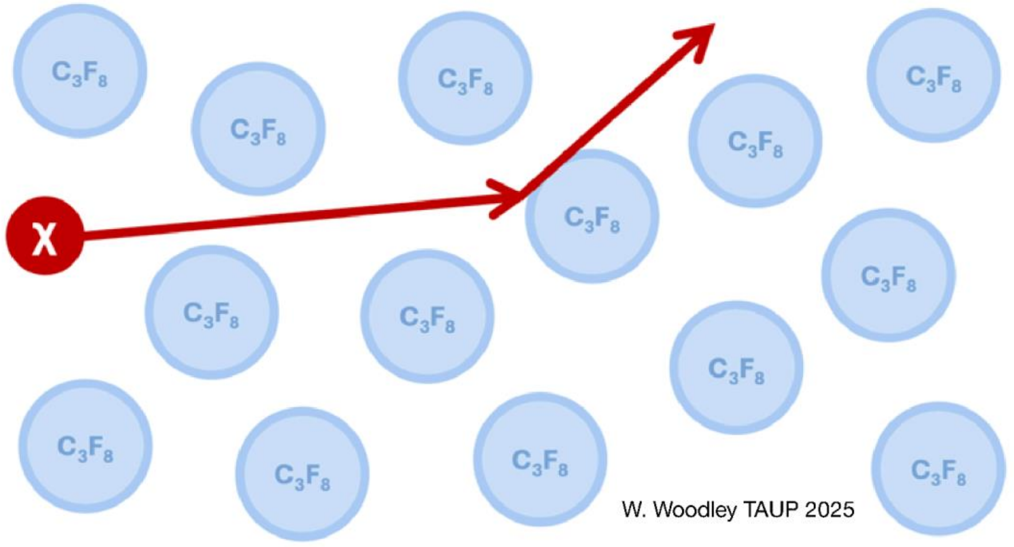

P, T tuned so WIMPs nucleate, ERs don't

The Physics of Bubble Nucleation

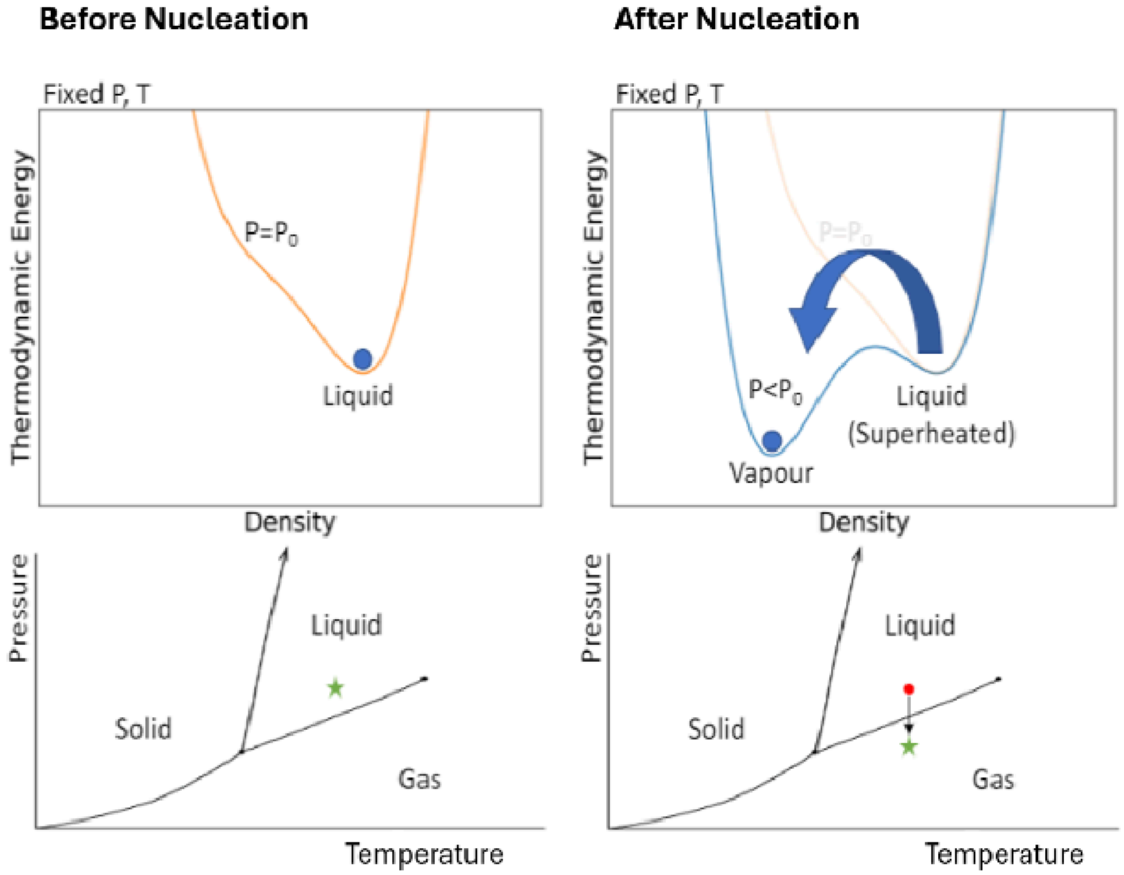

Critical radius:

$$r_c = \frac{2\sigma}{P_b - P_l}.$$

Seitz threshold energy:

Form the surface of a sphere | Convert liquid to sphere of vapour | Work done by expanding gas

$$Q_{\text{Seitz}} = 4\pi r_c^2\left(\sigma - T\frac{\partial\sigma}{\partial T}\right) + \frac{4\pi r_c^3}{3}\rho_b(h_b - h_l) - \frac{4\pi r_c^3}{3}(P_b - P_l)$$

A superheated liquid sits in a metastable minimum. Nucleation crosses the barrier to a lower-energy vapor state — the Gibbs free-energy cost of forming that critical bubble is exactly Q_{seith}.

Stopping Power: Why PICO is Blind to Electron Recoils

- Electrons (shaded band) deposit energy far too diffusely — their dE/dx sits well below the $^{12}C/^{19}F$ recoil curves and below the Seitz-threshold lines (dashed) at any energy.
- An electron recoil simply cannot concentrate enough energy within rc to cross Q_{seith} — no cut is needed, the physics does the rejection.
- ^{222}Rn and ^{218}Po alphas sit at the opposite extreme — very high dE/dx — which is why they nucleate so efficiently and ring louder acoustically.

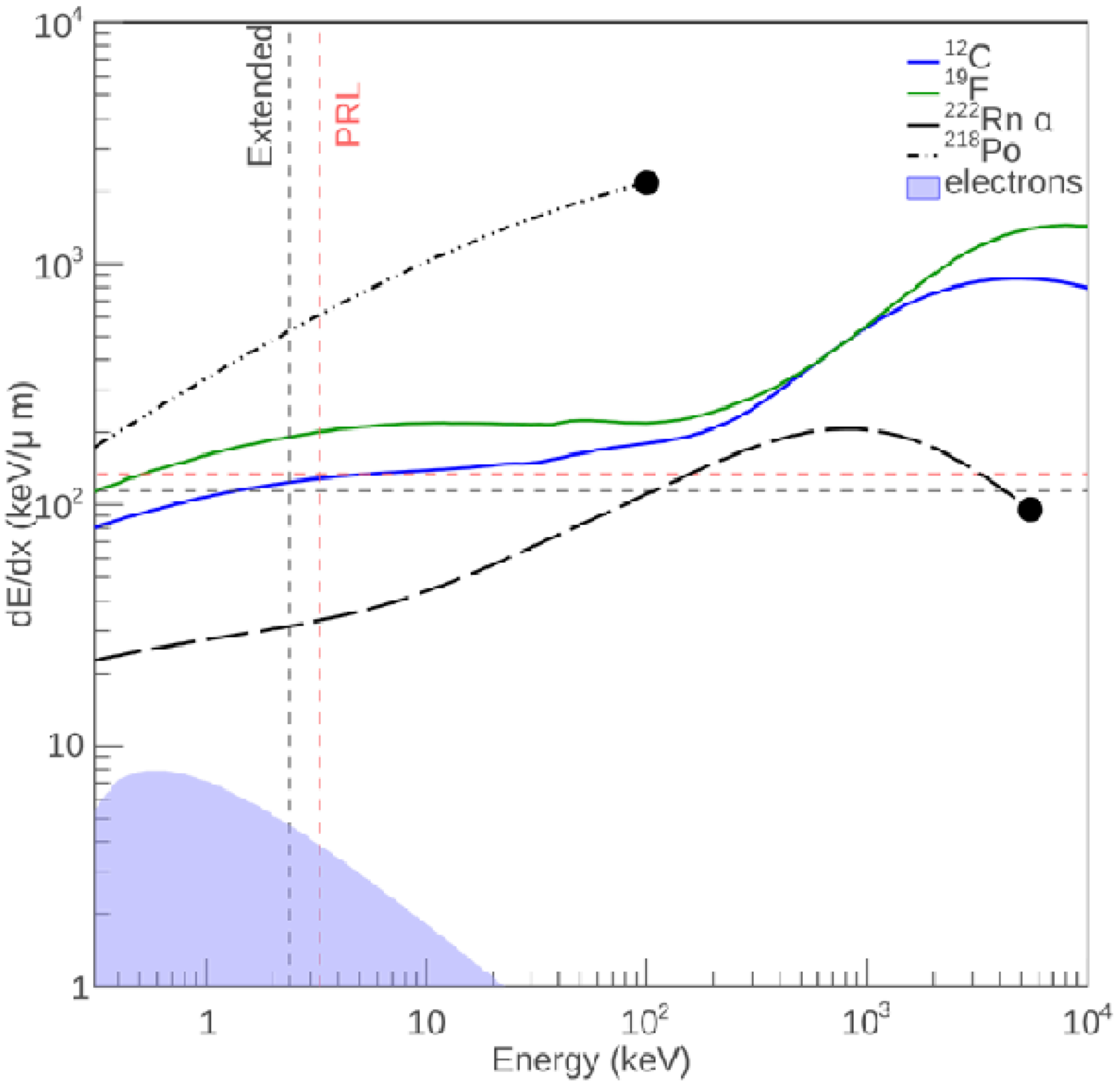

Nucleation Efficiency: Fluorine vs Carbon

- At a given Q_{seith}, fluorine turns on at lower recoil energy than carbon — F is the more efficient SD-sensitive nucleus in C_3F_8.
- Raising Q_{seith} from 2.45 to 3.29 keV shifts both turn-on curves right, trading nuclear-recoil acceptance for lower background.
- This efficiency curve is what converts a raw exposure into an effective WIMP exposure in the sensitivity plots.

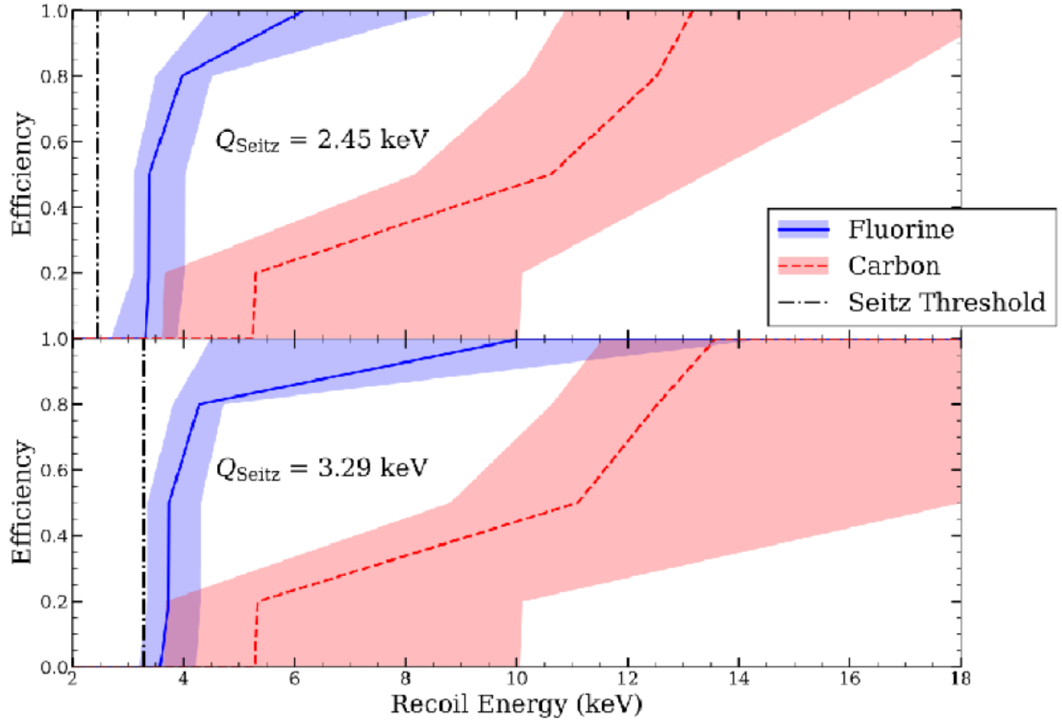

Figure 3.5: Nucleation efficiency for fluorine (solid blue) and carbon (dashed red), with their associated 1-σ uncertainty bands, at Q_{Seitz} = 2.45 keV (top) and 3.29 keV (bottom). Data is from [149].

Choosing the Operating Point

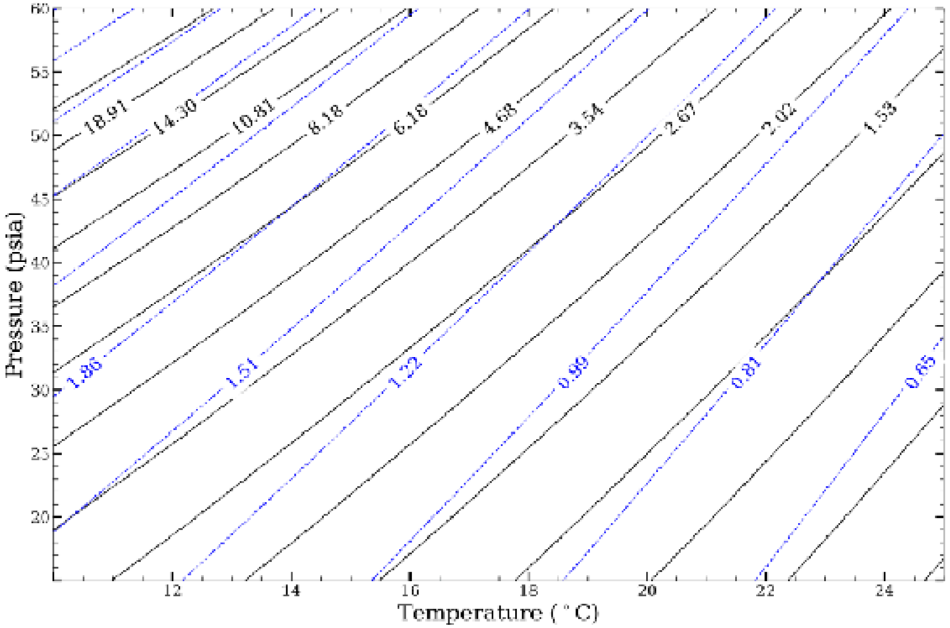

Q_{seith} (keV) contours vs. pressure and C_3F_8 temperature — pick the (P,T) that gives the desired threshold.

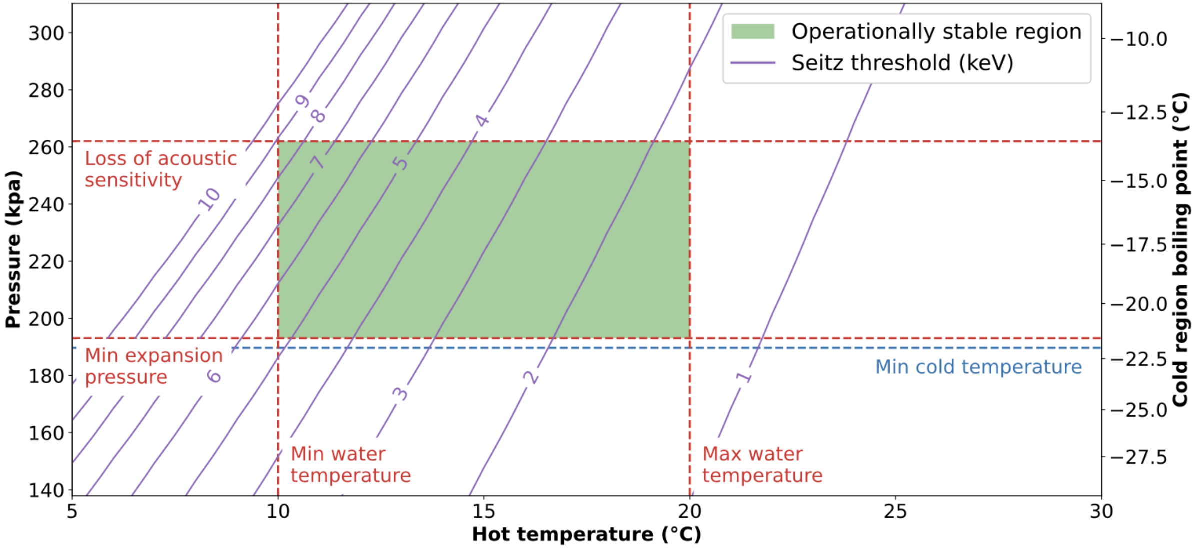

Left: Q_{seith} vs. C_3F_8 temperature for operating pressures 10–35 psia. Right: vapor-pressure curve with the actual PICO-40L operating point marked.

RSU Mechanics: Balancing Forces at the Bellows

- The bellows separates the hydraulic oil (actuation) from the C_3F_8 target plus a mechanical spring.
- Force balance: $F_{oil} = F_{C_3F_8} + F_{spring}$ — this sets the working pressure the piezo/Dytran system must operate around.
- Getting this balance right is what keeps the bellows itself from nucleating — a background source distinct from the walls.

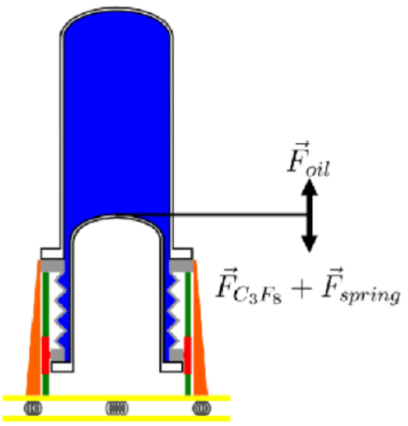

Figure 5.31: Free body diagram of the forces used in Equation 5.14.

Three Independent Detection Channels

- Acoustic — 12 piezoelectric transducers: record the pressure wave radiating from a forming bubble; alphas ring measurably louder than neutrons.
- Pressure — 2 Dytran transducers: track pressure rise vs. time; separate single- from multi-bubble events and flag wall nucleations.
- Optical — 4 cameras: trigger chamber recompression, provide 3D position reconstruction, define the fiducial volume.
- A WIMP candidate must pass all three: single bubble, neutron-like acoustically, inside the fiducial volume.

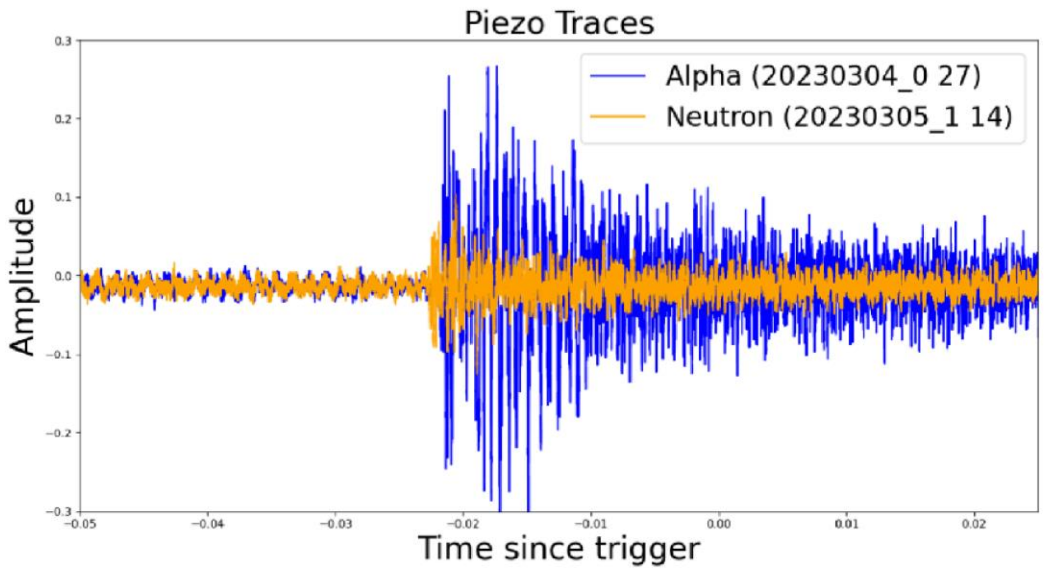

Acoustic waveform: alpha, radon-daughter, and neutron populations separate cleanly

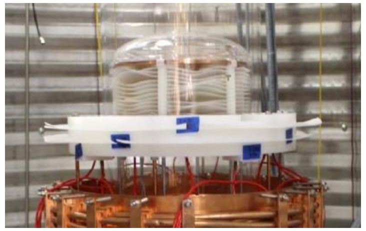

Piezo transducers (left) mounted on the PICO-40L instrumentation ring (right)

Optical Trigger: Frame-to-Frame Entropy

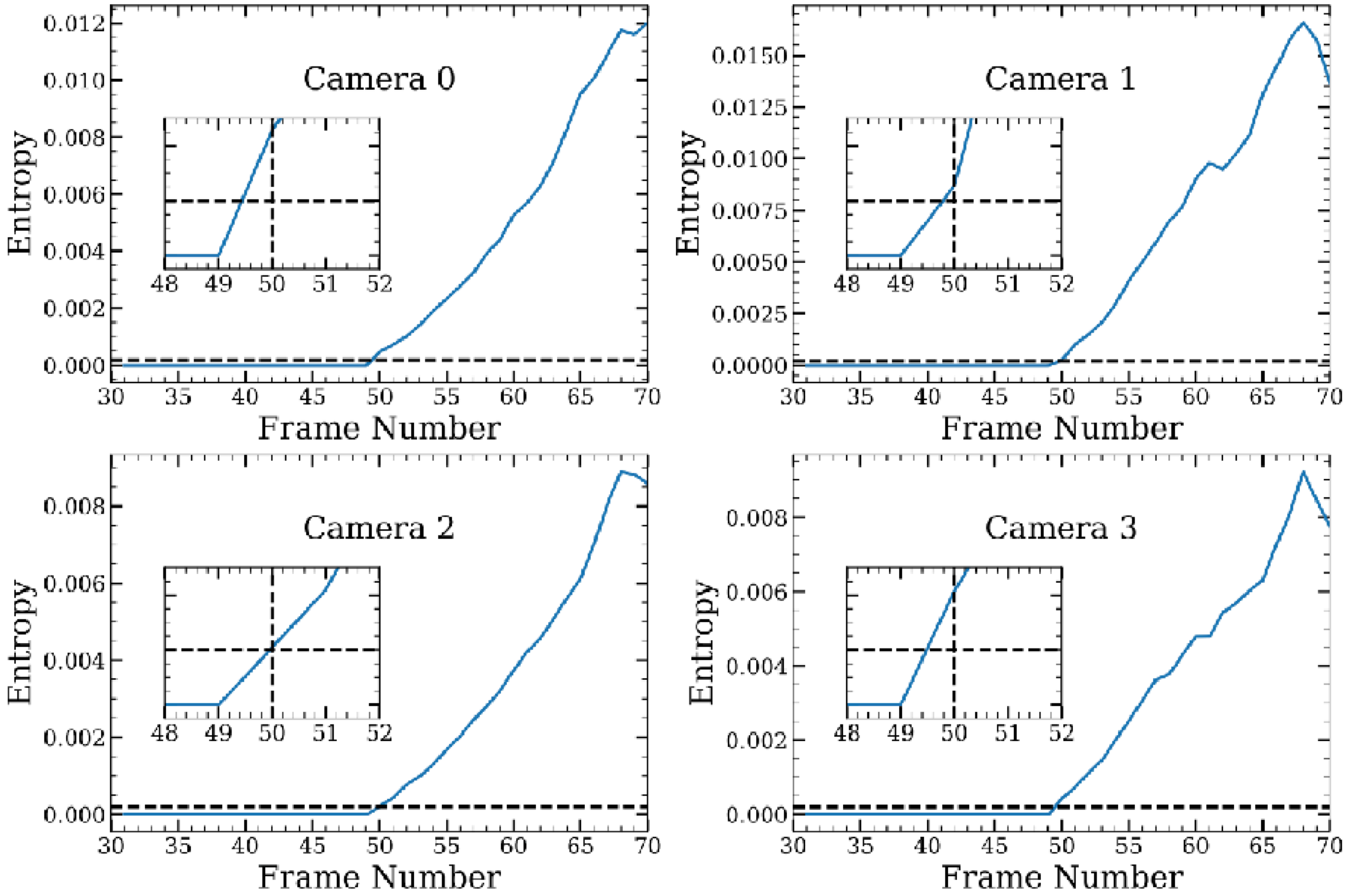

- Each camera watches frame-to-frame image entropy; a bubble appearing in the fluid causes a sharp jump.
- All four cameras cross the trigger threshold within ~1 frame of each other (inset), confirming a single, real event rather than a spurious glint.

Determining T0 from the Acoustic Signal

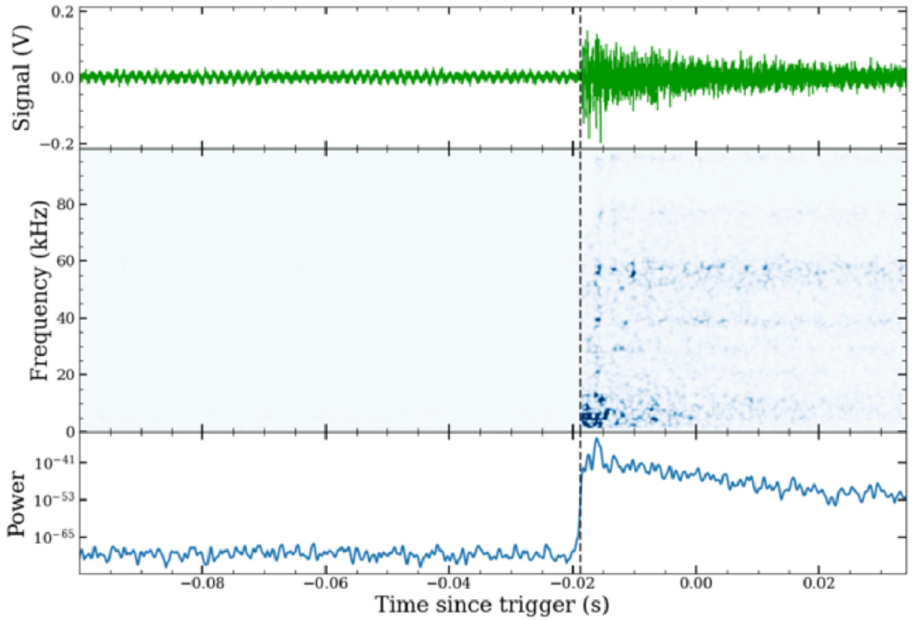

Figure 5.19: Combined plot of the steps to determine t0, with t0 shown on each plot in grey.

- T0 (nucleation time) is defined where the squared derivative of the piezo signal crosses a fixed threshold — visible in all three panels (raw signal, spectrogram, power).
- This acoustic T0 is cross-checked against the camera trigger frame, giving an independent timing handle for every event.

Computing the Acoustic Parameter (AP)

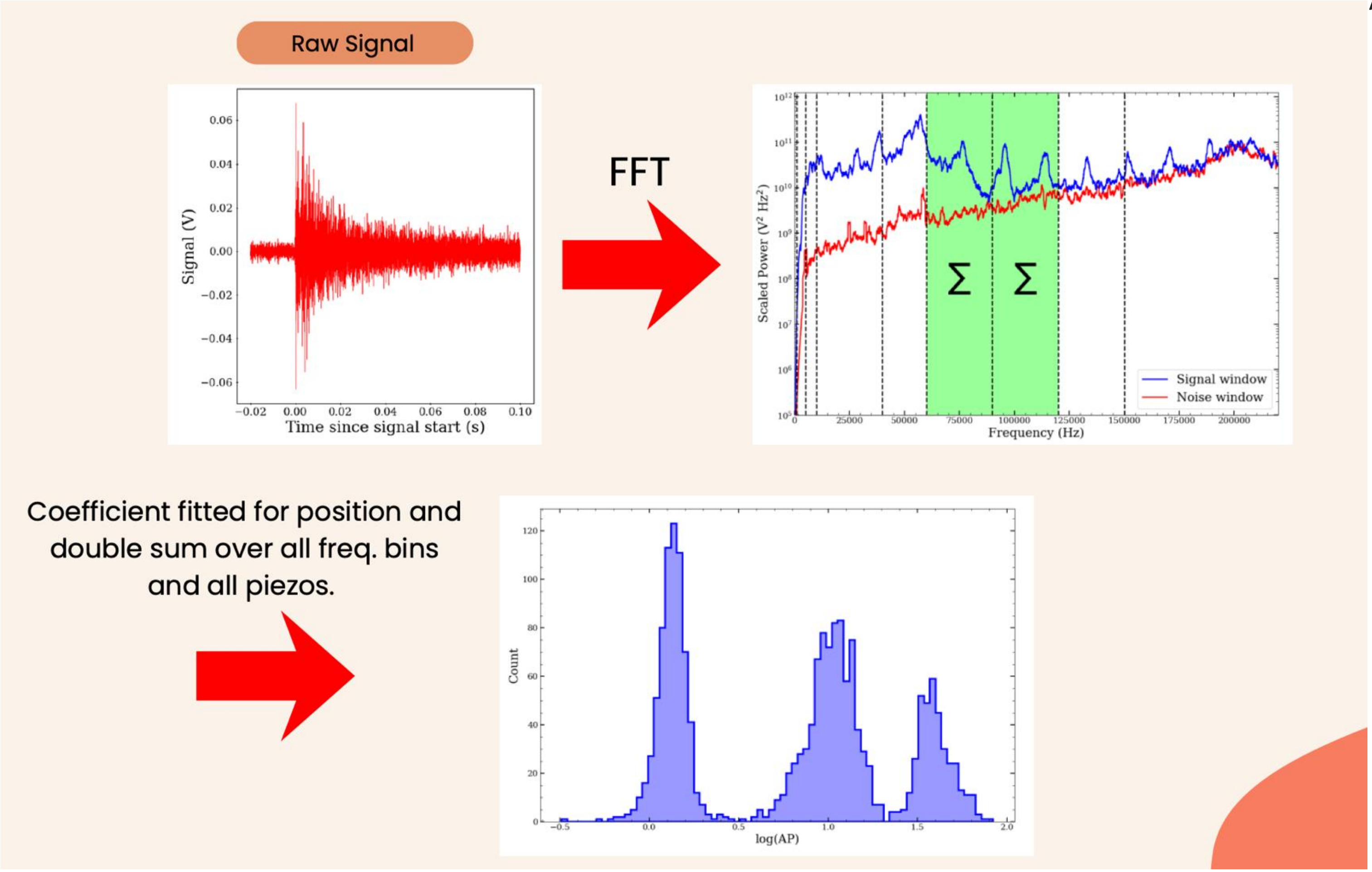

Credit: Jeremy Savoie

Per-piezo, per-band residual power S, R, then averaged into a single AP per event:

$$\mathcal{S}_{p,b} = \sum_{i=f_{b,1}}^{f_{b,2}} \mathrm{psd}_i \times f_i \,,$$

$$\mathcal{R}_{p,b} = \mathcal{S}_{p,b} - \mathcal{N}_{p,b} \,,$$

$$\mathrm{AP} = \frac{\sum_p \sum_{b=0}^{8} G(b) R^*_{p,b}}{\sum_p \sum_{b=0}^{8} G(b)} \,,$$

The Compression–Expansion Cycle

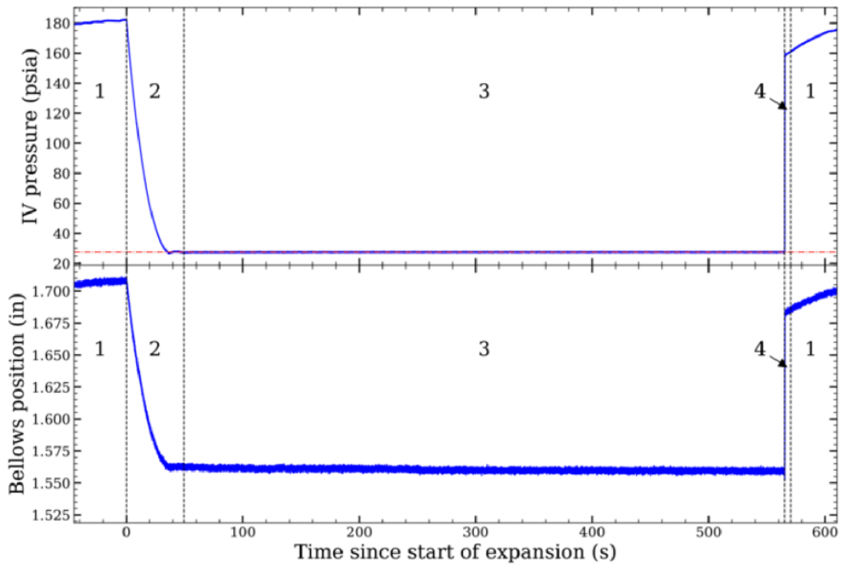

Figure 4.9: Pressure within the IV (top) and bellows distance from calibration point (bottom) versus time for a typical expansion. The vertical lines and inset numbers denote the different stages of a pressure cycle, as described in the text.

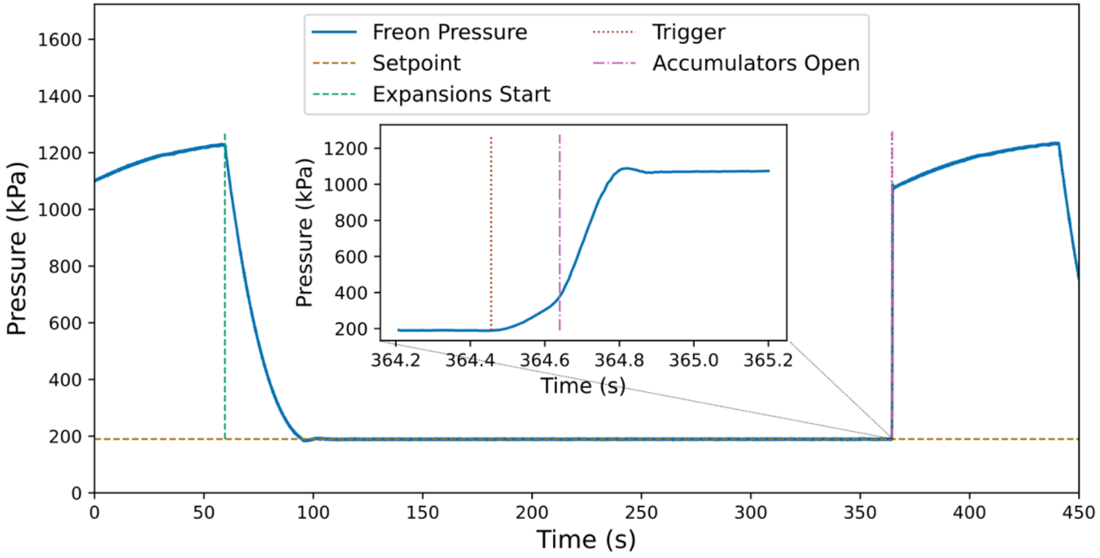

- Stage 1 — compressed, waiting between runs. Stage 2 — fast expansion into the superheated operating point.
- Stage 3 — live, superheated dead-time (up to several hundred seconds) where a WIMP or background event can nucleate a bubble.
- Stage 4 — a trigger fires and fast piston accumulators recompress the chamber in well under a second, ready for the next cycle.

Backgrounds — Identified and Suppressed

- Alphas (^{222}Rn/^{220}Rn chains): louder acoustically than neutrons — total rate 63.76 ± 1.46/day, rejected via AP.
- Neutrons: single:multi-bubble ratio of 1:3.3 lets us tag and constrain the internal neutron rate (sim.: 4.0±0.9 single, 9.3±2.2 multi bulk events).
- Gammas: insensitive at operating threshold — $(1.17\pm0.58)\times10^{-2}$ evts/live-yr.
- Neutrino floor (C_3F_8): 1.10 ± 0.10 evts/live-yr — among the lowest of any target fluid.
- Wall nucleations: faster, more violent growth than bulk events — identified via Dytran pulse shape + camera position and excluded from the fiducial volume.

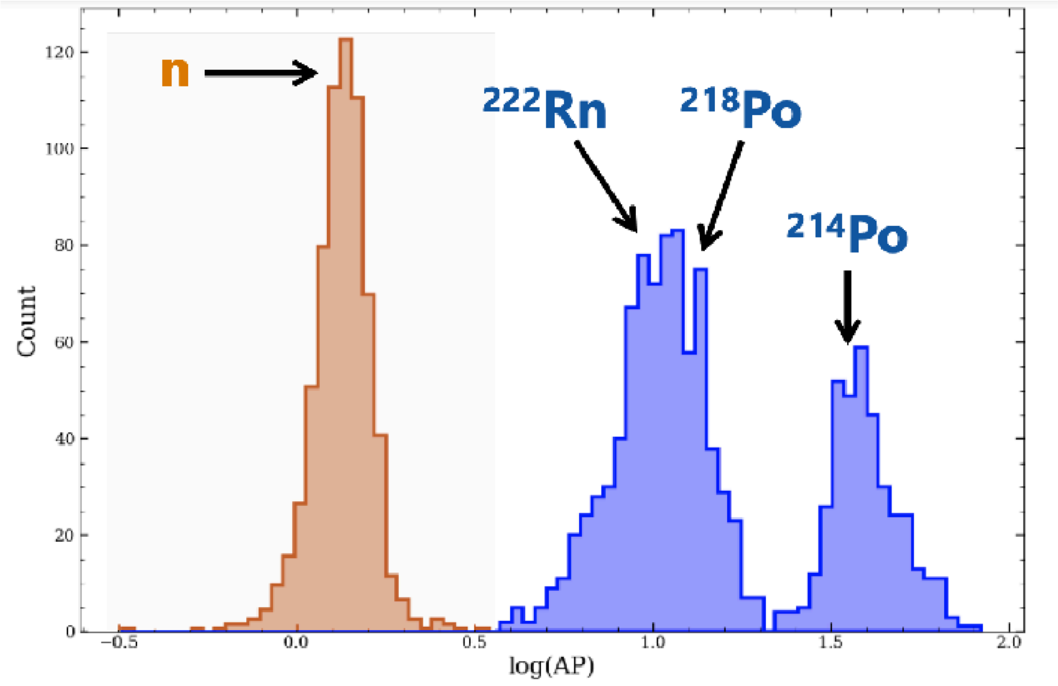

Acoustic parameter (AP) separates alpha, radon-daughter, and neutron populations

Material Radioassay: The Background Budget

Component	Single-Bubble Events per Live-Year
Mineral Oil	< 0.68
Inner Cu Disk	$0.10^{+0.11}_{-0.10}$
Outer Cu Plate	$0.08^{+0.10}_{-0.08}$
Lower Retroreflector	$\left(5.93^{+0.18}_{-0.16}\right) \times 10^{-2}$
Thermal Insulation	$< 1.26 \times 10^{-2}$
Upper Retroreflector	$\left(1.15^{+0.03}_{-0.03}\right) \times 10^{-2}$
Pressure Vessel	$< 1.14 \times 10^{-2}$
Cameras	$\left(7.8^{+0.6}_{-0.6}\right) \times 10^{-3}$
Inner RTDs	$\left(7.2^{+2.1}_{-2.1}\right) \times 10^{-3}$
Piezoelectric Copper Housing	$\left(6.6^{+4.6}_{-4.3}\right) \times 10^{-3}$
Piezoelectric PCB	$\left(2.0^{+1.0}_{-0.9}\right) \times 10^{-3}$
Outer Vessel	$\left(5.6^{+2.6}_{-2.5}\right) \times 10^{-4}$
Outer RTDs	$\left(5.4^{+1.6}_{-1.6}\right) \times 10^{-4}$
LED	$\left(4.2^{+1.4}_{-1.3}\right) \times 10^{-4}$
PZT Ceramic	$\left(6.2^{+1.7}_{-1.6}\right) \times 10^{-5}$
Inner Vessel	$\left(4.6^{+1.5}_{-1.5}\right) \times 10^{-5}$
Cosmogenic Neutrons	< 0.1
CEvNS	0.1
Electronic Recoil Events	0.1
Total	< 1.32

- Component-by-component radioassay converts each material's measured activity into a predicted single-bubble background rate.
- Dominant terms are the mineral oil buffer and the copper hardware (inner disk, outer plate) — each sub-event-per-year; retroreflectors, RTDs, cameras, and piezo components contribute far less.
- Combined material background is < 1.32 single-bubble events per live-year — comparable to, and safely below, the intrinsic CEvNS and electronic-recoil floors.

Energy Deposition Mechanisms & Bubble Multiplicity

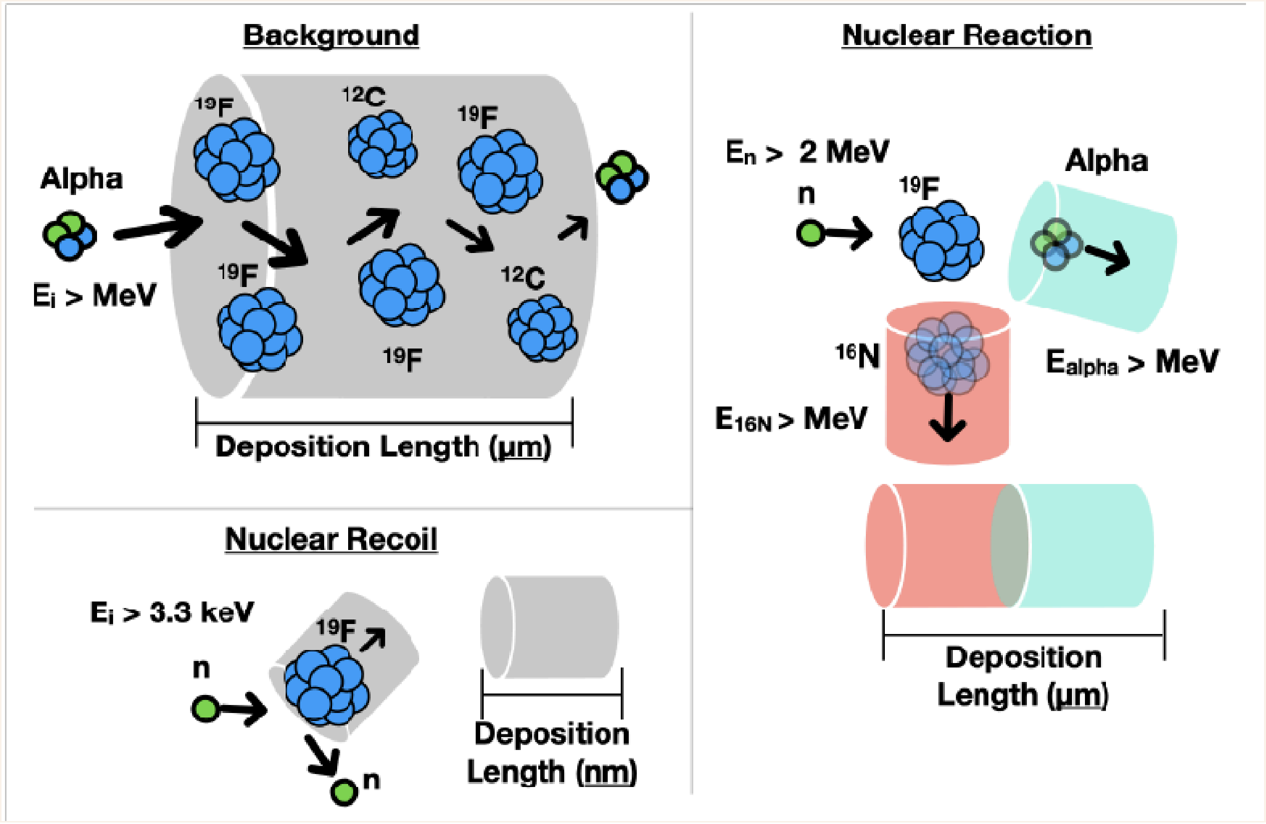

Different interaction channels deposit energy over very different length scales — this is what the chamber's threshold physics exploits.

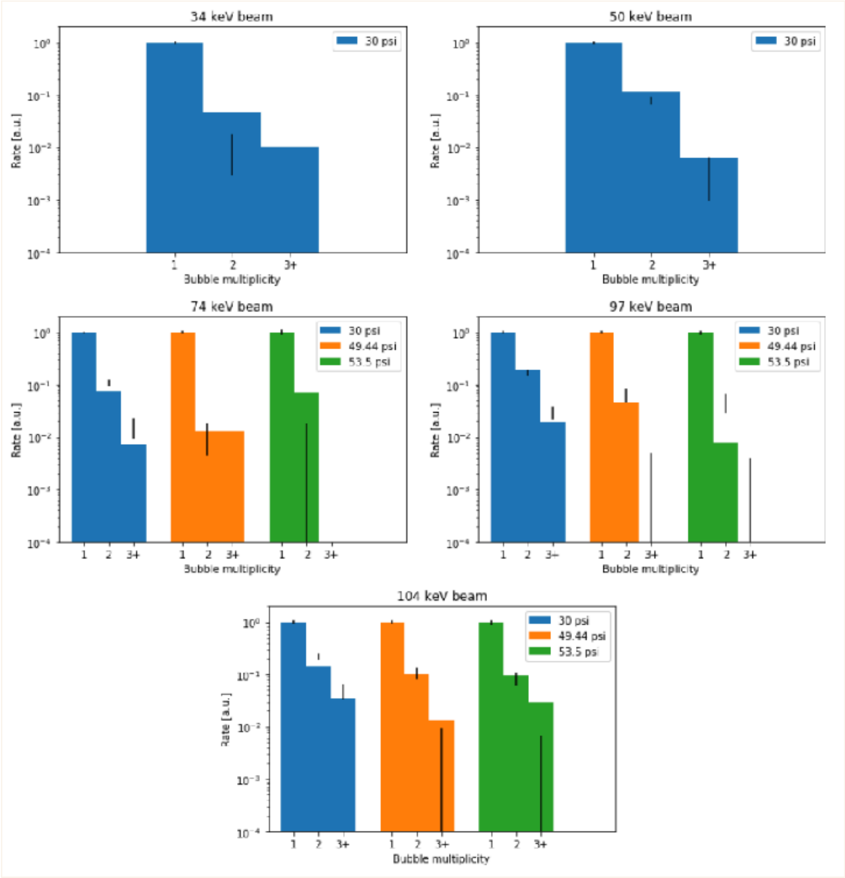

Multiplicity vs. incident neutron energy: single-bubble events dominate; higher energy beams give more multi-bubble events.

- Nuclear recoils deposit energy over nm-scale tracks near threshold; gammas/electrons spread energy over μm-scale tracks — the length-scale difference is exactly what sets the Seitz threshold's discriminating power.
- Single-bubble events are strongly favored at low incident energy; both threshold and beam energy govern the single:multi-bubble ratio used to constrain the internal neutron rate.

Wall-Event Rejection via the Dytran Signal

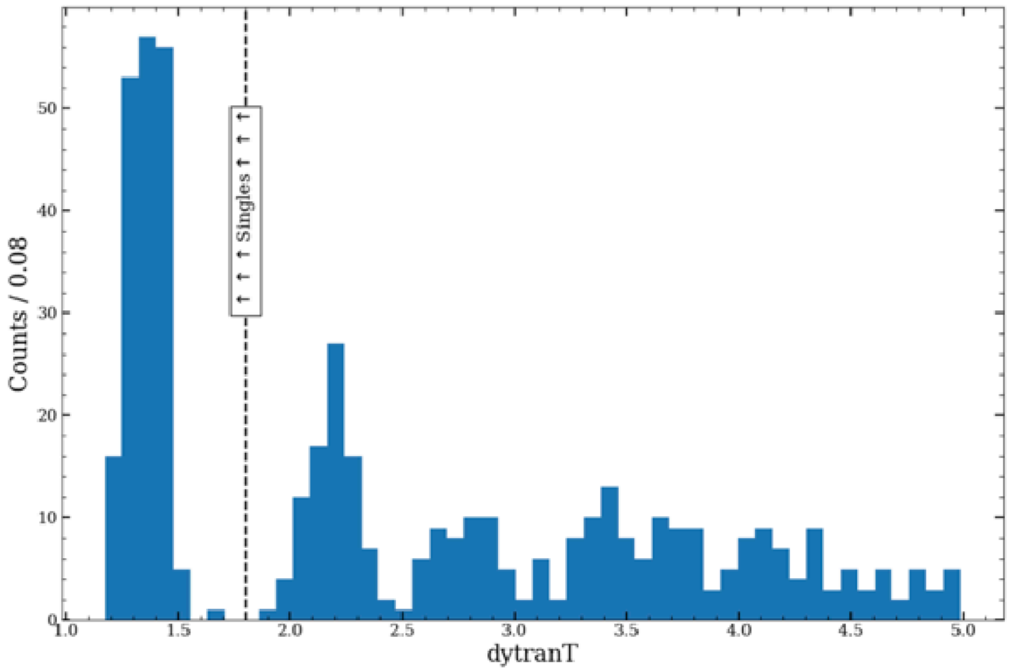

dytranT is bimodal: singles cluster low, walls cluster high of the cut threshold.

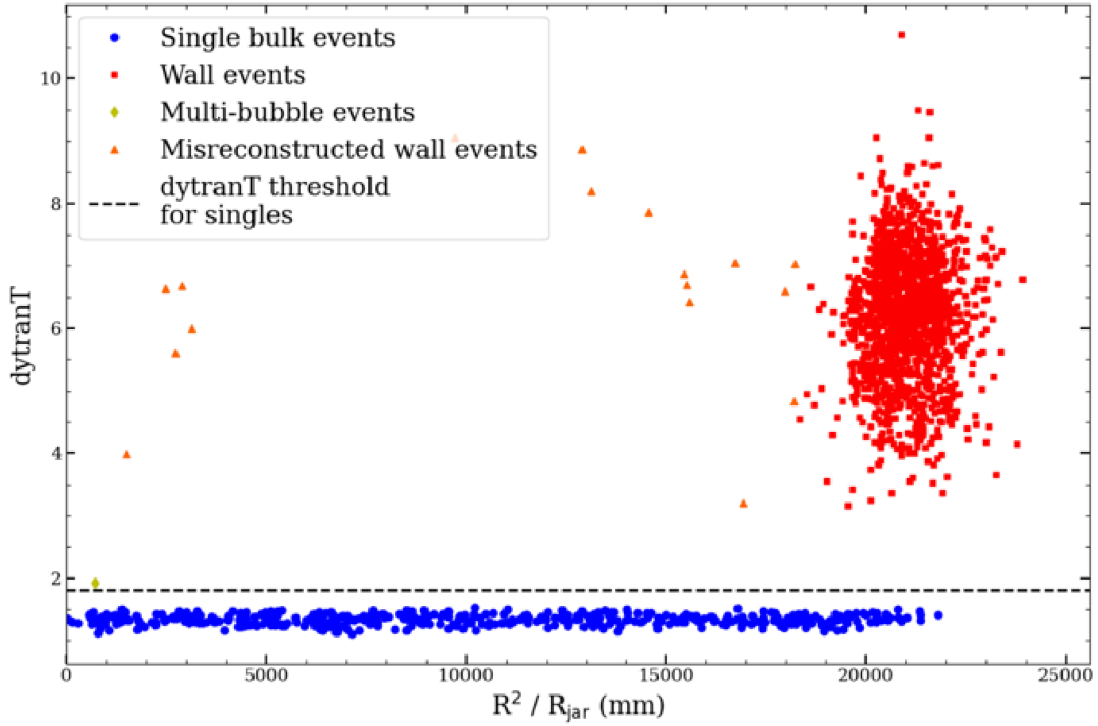

Position (R^2/Rjar) vs. dytranT: wall events sit at large radius with high dytranT; bulk singles sit low on both axes.

Internal Alpha Backgrounds: ^{238}U & ^{232}Th Chains

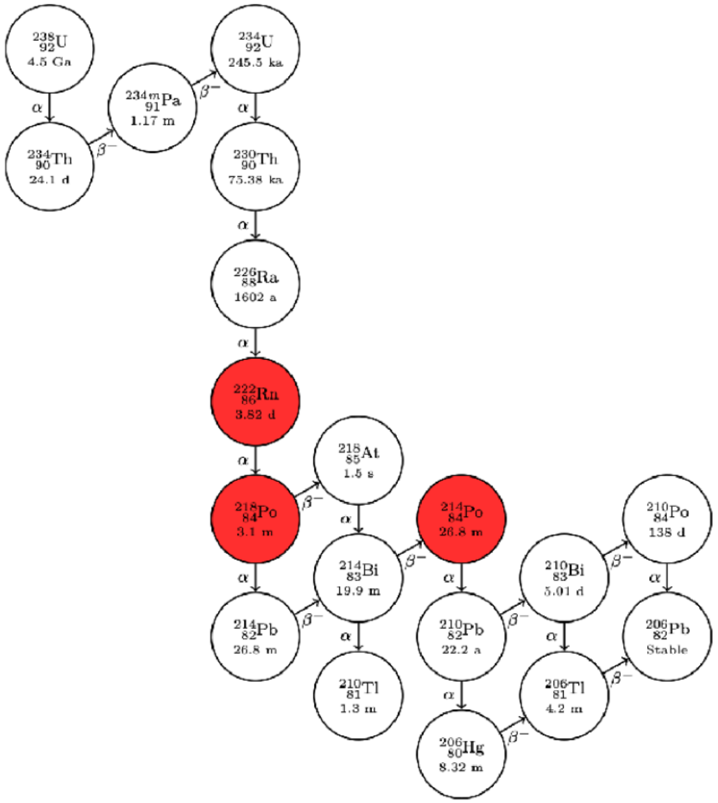

Figure 3.6: The uranium series. The elements in red are those which emit alpha particles, which are commonly observed in PICO-style detectors: ^{222}Rn (5.59 MeV), ^{218}Po (6.11 MeV), and ^{214}Po (7.83 MeV).

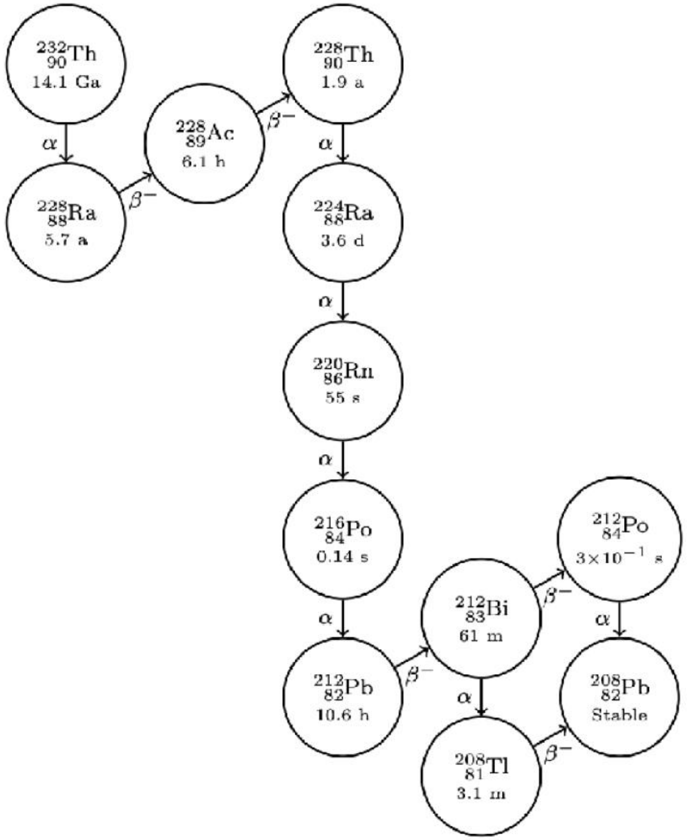

Figure 3.7: The thorium series.

^{222}Rn, ^{218}Po, and ^{214}Po (highlighted) from the ^{238}U chain, plus the analogous ^{232}Th-chain nuclides, are the intrinsic alpha emitters resolved on the AP spectrum.

Neutrino Backgrounds: Solar, Atmospheric, DSNB

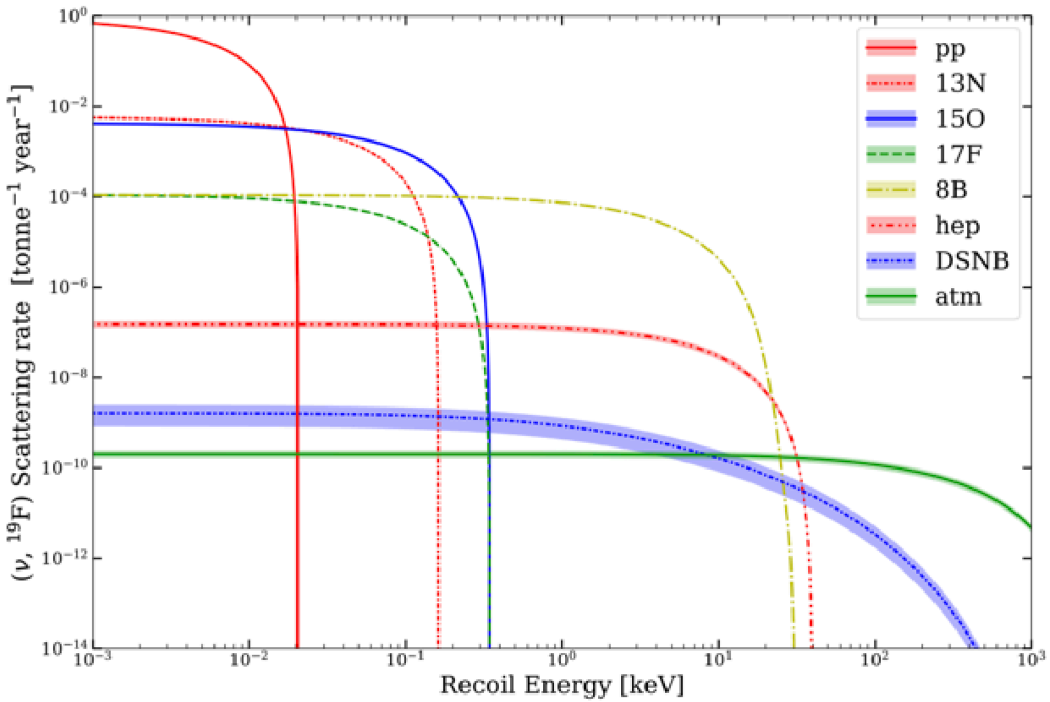

(ν, ¹⁹F) scattering rate — the dominant nucleus for SD sensitivity.

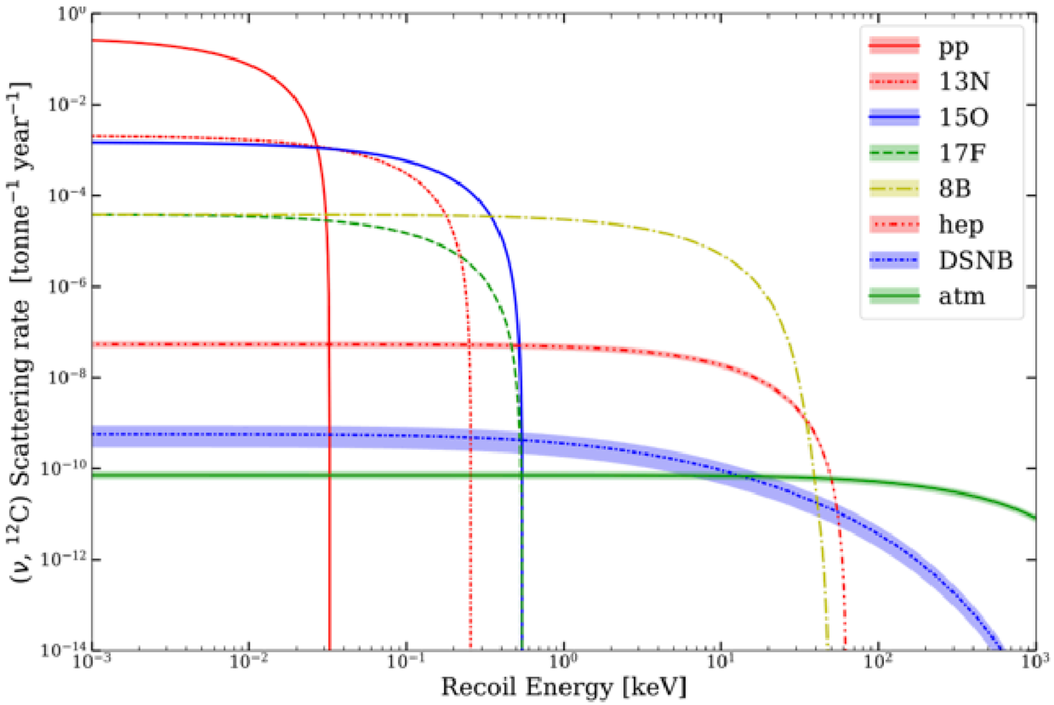

(ν, ¹²C) scattering rate for comparison.

pp solar neutrinos dominate sub-keV recoils; ^{8}B/hep contribute at the few-keV scale; atmospheric ν + DSNB set the irreducible floor at higher threshold.

The Neutrino Floor: Expected CEvNS Rates

Differential CEvNS cross section:

$$\frac{d\sigma_\nu}{dE_r} = \frac{G_F^2}{4\pi} Q_w^2 \, m_N \left(1 - \frac{m_N E_r}{2E_\nu^2}\right) F^2(E_r)\,,$$

Threshold (keV)	Fiducial Mass (kg)	Neutrino Rate (cts/live year)
3.29	45.33	1.10 ± 0.10
3.29	364.0	$8.85^{+0.86}_{-0.78}$
8.2		$0.98^{+0.27}_{-0.21}$
10		$0.42^{+0.15}_{-0.12}$

Table 6.13: Rate of CEνNS events per live year for PICO-40L (top row) and PICO-500 (bottom three rows).

- PICO-40L (45.3 kg, 3.29 keV threshold): 1.10 ± 0.10 CEvNS counts per live-year — already an appreciable fraction of the total background budget.
- PICO-500 (364 kg fiducial mass) trades threshold for rate: 8.85 cts/yr at 3.29 keV, falling to 0.98 at 8.2 keV and 0.42 at 10 keV — a direct exposure-vs-neutrino-floor design choice.

Alpha Spectroscopy: A New Bubble-Chamber Capability

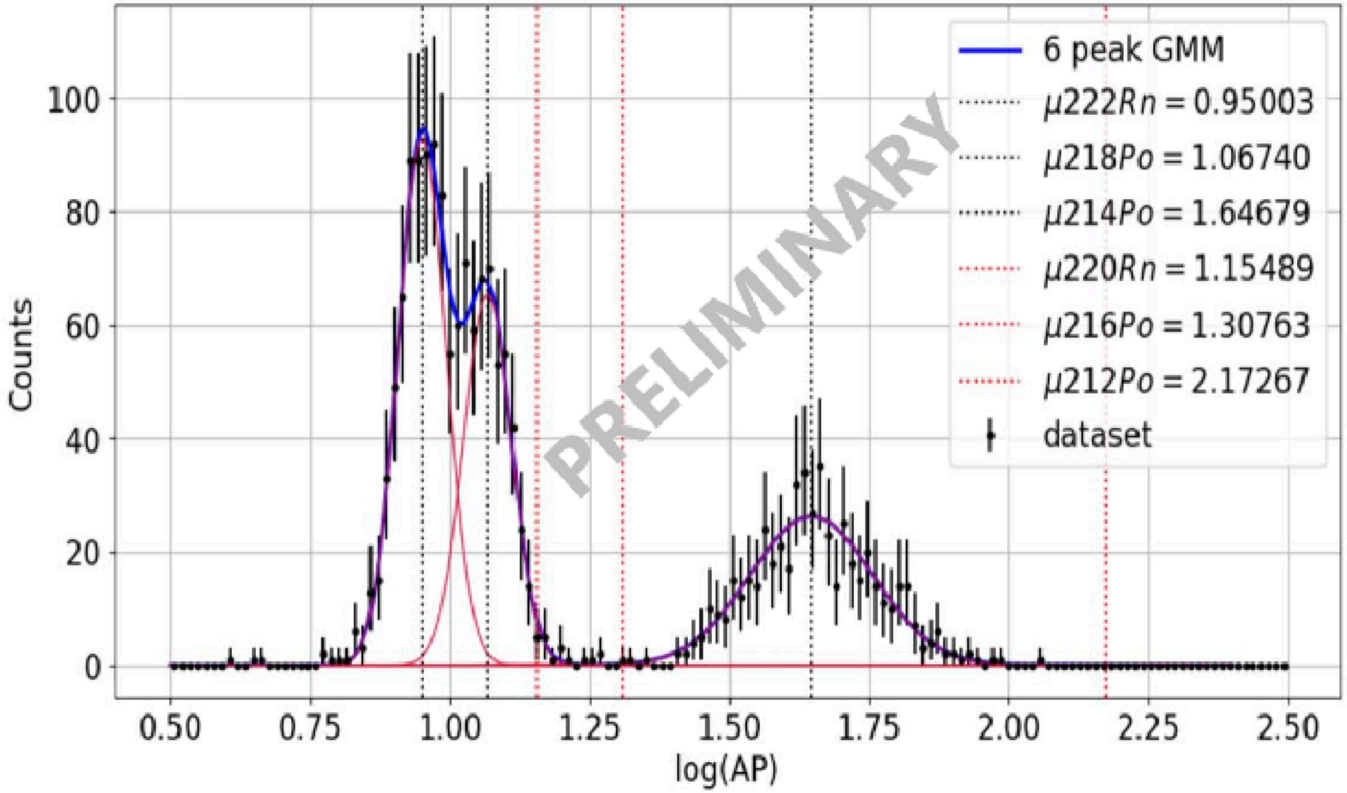

- Six distinct alpha lines resolved directly from the AP fit: ^{222}Rn, ^{218}Po, ^{214}Po and their ^{232}Th-chain analogues ^{220}Rn, ^{216}Po, ^{212}Po.
- Preliminary result — paper in preparation. This is, to our knowledge, the first in-situ acoustic alpha spectroscopy performed in a bubble chamber.
- Beyond a physics result, it's a built-in radioassay tool: PICO can fingerprint its own U/Th contamination directly from science data.

Global Landscape: SD-Proton vs SD-Neutron

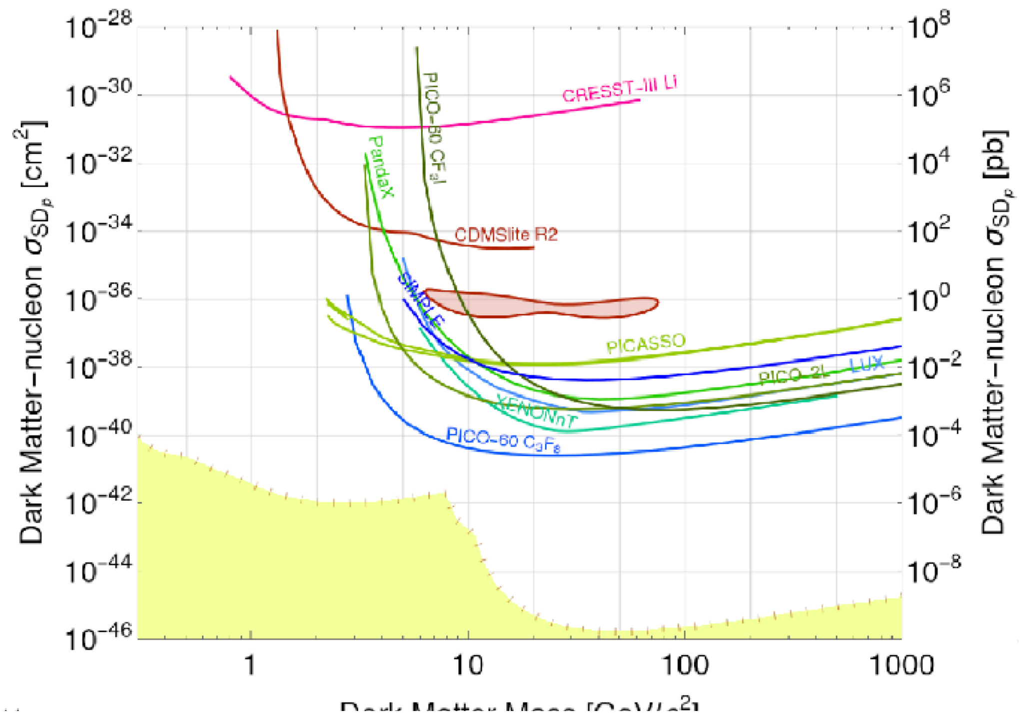

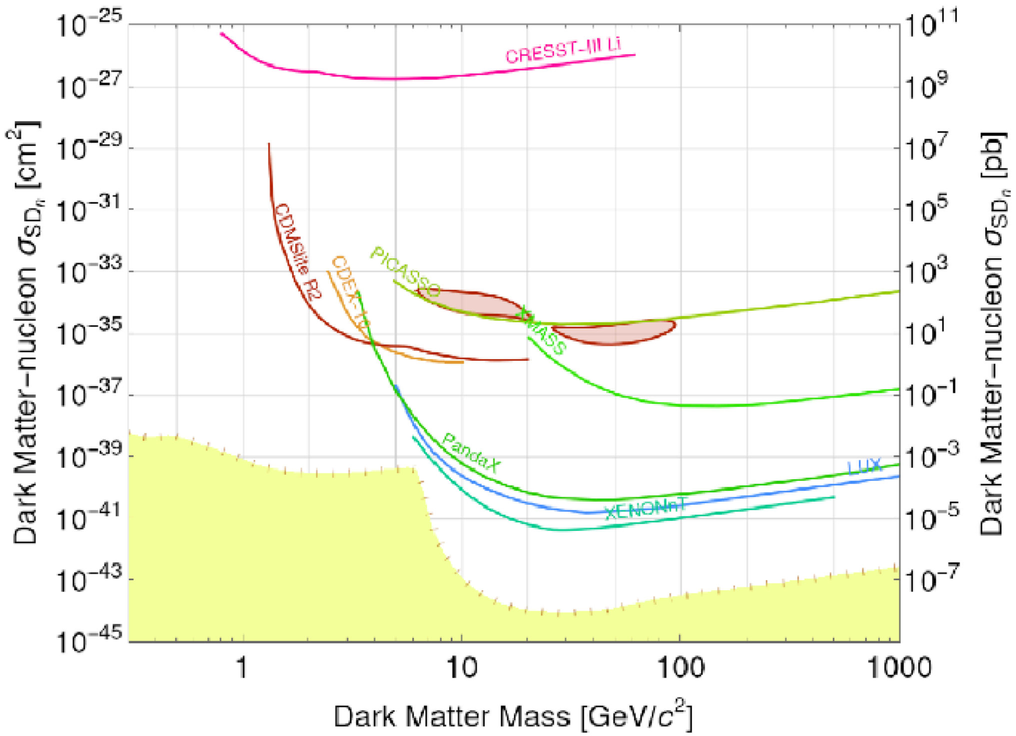

σ_SDn: xenon experiments (LZ, XENONnT, PandaX) lead — unpaired-neutron sensitivity.

σ_SDp: PICO-60/2L and PICASSO lead — fluorine's large proton spin coupling.

PICO's niche is specifically the proton-coupled SD channel

For Completeness: The Spin-Independent Landscape

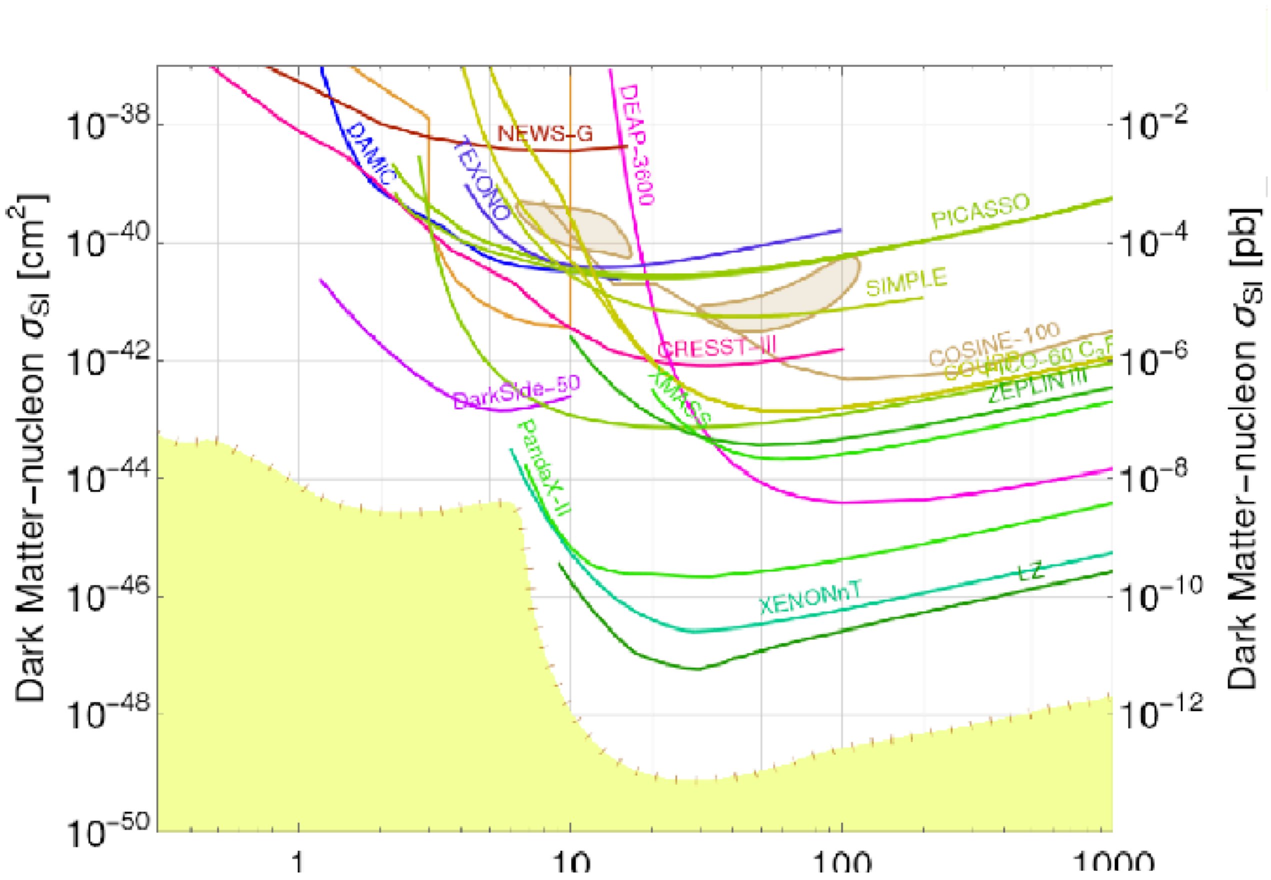

PICO is not competitive on σ_SI (∝A²) against Xe/Ge targets - light nuclei are simply outmatched.

Radon Assay Technique: Trap System & Flow Rate

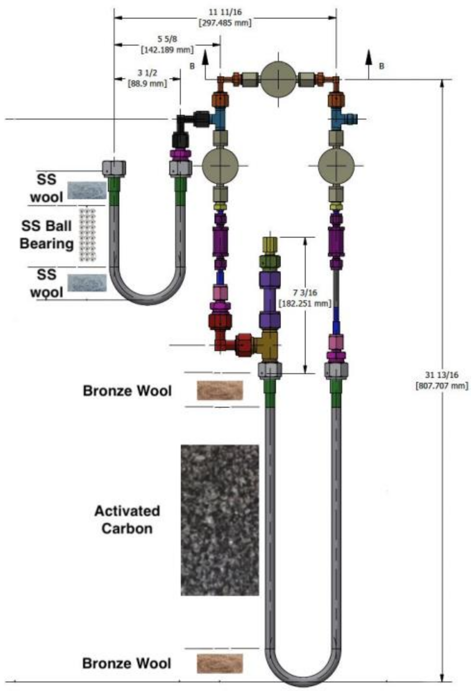

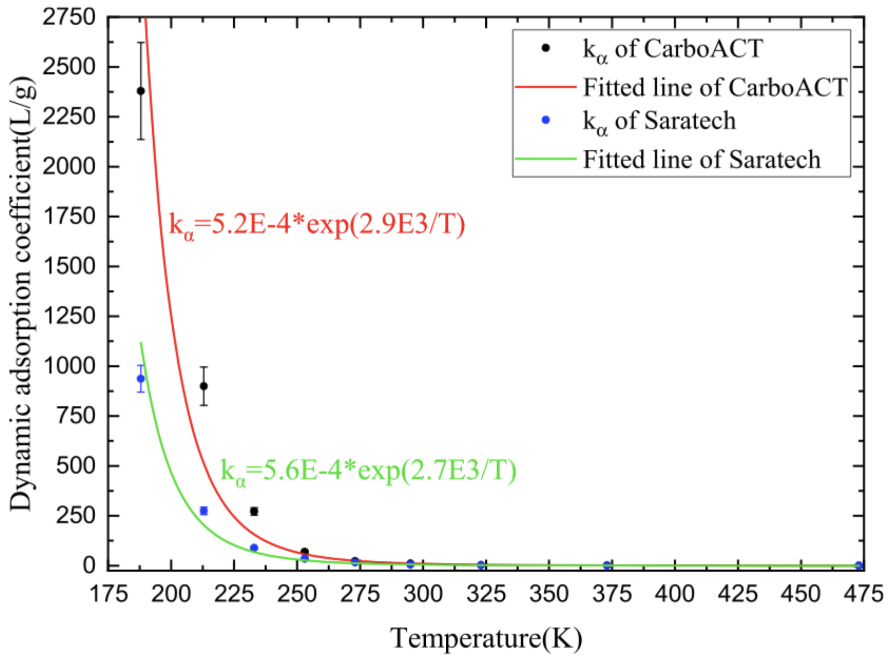

- Hybrid pre-concentration train: water trap (SS ball + SS wool) removes moisture; Rn trap (bronze wool + ~15.3 ± 0.3 g activated charcoal) adsorbs radon.
- 0.5 SLPM chosen to maximize the dynamic adsorption coefficient K_a (rises exponentially as trap temperature drops, right), keeping breakthrough time $\tau = K_a \cdot m/Q$ far longer than the ~1 hr counting window.
- Trapped radon is cryogenically released and transferred to a calibrated Lucas cell for alpha counting.

Radon Assay Technique: Campaign & Data Quality

- Seven emanation runs carried out May–July 2026 on two calibrated Lucas cells (background rates measured and subtracted separately for each cell).
- Three runs (1st, 4th, 7th) returned good statistics with mutually consistent rates; others were compromised by hardware issues — an open valve, a DAQ power interruption, a fitting leak — and are excluded from the quoted result.
- Dilution correction: only part of the emanated volume passes through the trap during a finite assay, so raw counts are scaled to a true rate via Ct = C0·exp(−Vpurge/Vcylinder), shown at right for a 250 L vessel.

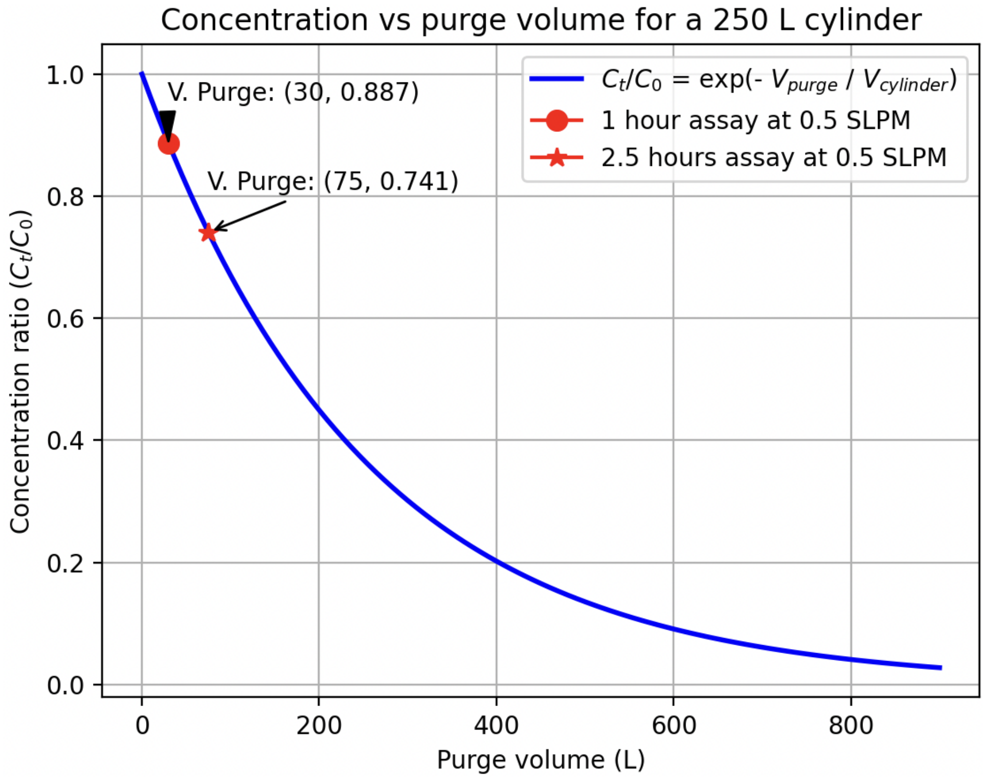

Radon Assay Technique: The Cryo-Trap in Operation

The hybrid trap's charcoal stage submerged in LN_2 during cryo-adsorption.

- The charcoal trap is held in a liquid-nitrogen dewar during cryo-adsorption, maximizing radon retention before counting.
- After the emanation period, the trap is warmed and the collected radon released into the counting line.
- This cryo step is what allows the assay to reach few-Bq sensitivity on a large (250 L-class) emanation volume.

Radon Assay Technique: From Emanation to Background Budget

- Seal permeation (independent cross-check): applying Fick's-law permeation through the elastomer seal, with the partial-pressure difference set by typical ambient Rn-222 activity, gives a permeation contribution well below the intrinsic emanation term — ingress through seals is not the dominant pathway.
- Radon-induced neutron background: alpha decays in the Rn-222/Rn-228 chains can drive (α,n) / (α,p) reactions in the bulk silica at branching ratios of order 10^{-5}.
- Folding the measured decay rate through this branching ratio projects a sub-dominant, order-0.1-events/year contribution — consistent with the radon-chain line already shown in the total background budget.

Numeric check pending — verify the decays/day vs. decays/year normalization and the (α,n) branching-ratio arithmetic with the analysis author before quoting a final number externally.

Fused-Silica Jar Screening

Q Why does the jar set a background floor that other components of similar mass do not?

It is in direct contact with the C_3F_8. Alphas and (α,n) neutrons born in the jar wall reach the active volume with no shielding, and wall events cannot be fiducialized away the way distant material can be.

Q Is a crushed sample representative of the installed jars?

The assayed material comes from the same production run as the installed jars, and the result is quoted as an upper limit rather than a central value, so run-to-run variation is absorbed into the bound we carry.

Q Does the crushed-sample assay say anything about the surface?

No. It bounds bulk U/Th/K only. Surface radon daughters are a separate problem, controlled by vessel cleaning and the continuous N_2 purge, slides 14 and 15.

Component Screening and the Material Budget

Q What exactly is inside the 1.14 single-bubble events per live-year?

The summed predicted rate from every screened component at the WIMP-search threshold. Where an assay returned a non-detection, its upper limit is carried, so the number is a bound rather than a central value.

Q Why do the mineral oil and the copper hardware dominate?

Mass and proximity. The oil buffer is the largest wetted mass, and the copper inner disk and outer plate sit closest to the active volume, so their neutron yield weighs most heavily in the sum.

Q How does a measured activity become a predicted bubble rate?

Measured U/Th/K activities feed a neutron production and transport simulation of the as-built geometry, and the result is folded with the nucleation efficiency at the operating threshold.

Radon Mitigation and Exposure Accounting

Q Why a continuous purge rather than a sealed bag or a vacuum?

Radon emanates from the jar itself and diffuses through the bag film, so a static seal lets it build up and plate out. Continuous flow sweeps it away before the daughters can deposit on a wetted surface.

Q How much radon exposure is left, and how is it accounted for?

Every interval without active flush is logged as exposure time. Exposure time multiplied by the ambient radon activity gives the plate-out estimate that is carried into the surface-alpha budget.

Q How do you know a bag never quietly lost its purge?

Daily N_2-sensor leak checks and dewar level and flow-rate logs at every stage. A drop in flow is recorded as an exposure event rather than assumed harmless.

Vessel Cleaning and Verification

Q Does cleaning remove plated-out Pb-210?

No. Pb-210 implanted in the surface survives any rinse, which is why exposure control matters more than cleaning for the long-lived daughters. Cleaning targets dust and loosely bound activity that drive wall nucleation.

Q How is cleanliness verified rather than assumed?

The outlet filter is photographed under a microscope and particulates are counted for each rinse. Rinsing continues until the count stops falling, and cleanroom particulate levels are logged daily.

Q Why Class 1000, and why clean the inner vessel underground?

Class 1000 holds deposition between cleaning and assembly below the wall-event budget. Cleaning the inner vessel underground removes the chance of re-contaminating it in transit after the final rinse.